Since January 2020 Elsevier has created a COVID-19 resource centre with free information in English and Mandarin on the novel coronavirus COVID-19. The COVID-19 resource centre is hosted on Elsevier Connect, the company's public news and information website.

European Journal of Radiology 131 (2020) 109217

Contents lists available at ScienceDirect

European Journal of Radiology

journal homepage: www.elsevier.com/locate/ejrad

Review

Multimodality imaging of COVID-19 pneumonia: from diagnosis to follow-up. A comprehensive review

Anna Rita Larici [a,b,c], Giuseppe Cicchetti [a,b,c], Riccardo Marano [a,b,c,*], Biagio Merlino [a,b,c], Lorenzo Elia [c], Lucio Calandriello [a,b], Annemilia del Ciello [a,b], Alessandra Farchione [a,b], Giancarlo Savino [a,b], Amato Infante [a,b,d], Luigi Larosa [a,b,d], Cesare Colosimo [a,b,c], Riccardo Manfredi [a,b,c], Luigi Natale [a,b,c]

[a] Department of Diagnostic Imaging, Oncological Radiotherapy, and Hematology – Diagnostic Imaging Area, Italy
[b] Fondazione Policlinico Universitario Agostino Gemelli IRCCS, Rome, Italy
[c] Università Cattolica del Sacro Cuore, Rome, Italy
[d] Columbus Covid 2 Hospital, Rome, Italy

ARTICLE INFO

Keywords:
COVID-19 pneumonia
Chest X-ray
High-resolution computed tomography
Diagnosis
Differential diagnosis
Follow-up

ABSTRACT

Due to its pandemic diffusion, SARS- CoV-2 (Severe Acute Respiratory Syndrome Coronavirus 2) infection represents a global threat. Despite a multiorgan involvement has been described, pneumonia is the most common manifestation of COVID-19 (Coronavirus disease 2019) and it is associated with a high morbidity and a considerable mortality.

Especially in the areas with high disease burden, chest imaging plays a crucial role to speed up the diagnostic process and to aid the patient management.

The purpose of this comprehensive review is to understand the diagnostic capabilities and limitations of chest X-ray (CXR) and high-resolution computed tomography (HRCT) in defining the common imaging features of COVID-19 pneumonia and correlating them with the underlying pathogenic mechanisms. The evolution of lung abnormalities over time, the uncommon findings, the possible complications, and the main differential diagnosis occurring in the pandemic phase of SARS-CoV-2 infection are also discussed.

1. Introduction

Severe Acute Respiratory Syndrome Coronavirus 2 (SARS-CoV-2) infection, named COVID-19 (coronavirus disease 2019), represents an epoch-making global healthcare crisis, with more than 696.000 deaths caused to date (August 6, 2020) worldwide [1].

Although COVID-19 may present as a multiorgan disease, the lung represents the most commonly affected target organ. Clinical manifestations may vary from flu-like symptoms, such as fever, dry cough, myalgia and fatigue, often coupled with hypo-/anosmia and ageusia [2–4], to more severe conditions with dyspnoea and respiratory impairment requiring admission to intensive care unit (ICU) and advanced respiratory assistance [5]. A severe course of the disease has been reported in 5–22 % of COVID-19 patients in published studies from various geographical areas [3,5].

In this scenario of medical emergency, chest imaging assumes a pivotal role in the triage and management of patients with confirmed or suspected COVID-19 pneumonia.

In this comprehensive review, which arises from the experience gained at our large tertiary care hospital during the SARS-CoV-2 outbreak in Italy and the available literature, we aim to describe the role of chest X-ray (CXR) and high-resolution computed tomography (HRCT) in the assessment of COVID-19 patients and to report the most common imaging features of COVID-19 pneumonia with a descriptive correlation to the underlying pathogenesis. We also report the spectrum of lung abnormalities at follow-up imaging and discuss possible uncommon imaging findings, complications and differential diagnosis with a case- based approach to increase the diagnostic awareness of radiologists.

* Corresponding author at: Department of Diagnostic Imaging, Oncological Radiotherapy, and Hematology – Diagnostic Imaging Area, Fondazione Policlinico Universitario Agostino Gemelli IRCCS, Università Cattolica del Sacro Cuore, L.go Agostino Gemelli 8, Rome 00168, Italy.
E-mail address: riccardo.marano@unicatt.it (R. Marano).

https://doi.org/10.1016/j.ejrad.2020.109217
Received 22 May 2020; Accepted 12 August 2020
Available online 17 August 2020
0720-048X/

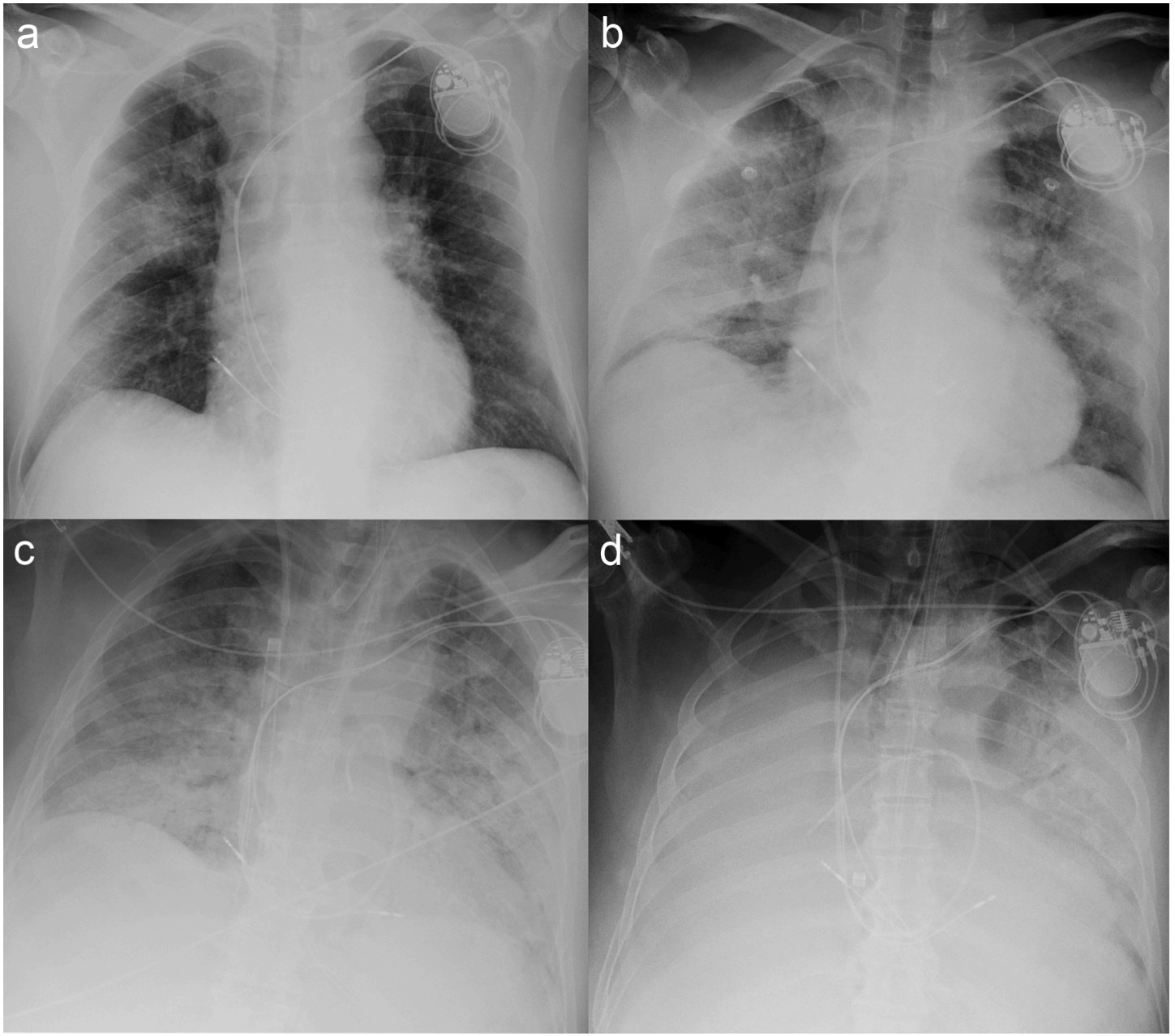

Fig. 1. Worsening evolution of COVID-19 pneumonia in a 63- year-old male with known cardiac disease (note the presence of a pacemaker). The first antero-posterior (AP) chest X-ray (CXR) (a) shows hazy opacities with a mid-basal and peripheral predominance on the right lung, without pleural effusion. Two days later, the AP CXR (b) depicts confluent and bilateral alveolar opacities with air bronchogram and quite diffuse distribution. CXR performed 9 days later in ICU (c) shows a further increase of bilateral alveolar opacities, especially in the mid-basal lungs. In the last CXR (d), a further radiographic worsening was evident, with development of bilateral "whited lung". The patient deceased two days later due to ARDS.

2. Diagnosis of COVID-19 pneumonia: the potential role of chest imaging

Chest imaging can provide rapid and valuable information in the diagnosis of COVID-19 pneumonia [6].

The reference standard for the diagnosis of COVID-19 infection is the identification of viral RNA by the real-time reverse transcriptase polymerase chain reaction essay (RT-PCR) of respiratory secretions obtained by nasopharyngeal and/or oropharyngeal swab or bronchoalveolar lavage (BAL). However, the sensitivity of this test ranges from 32 % to 71 %, depending on the stage and severity of the disease, specimen handling, and swab type [7–9]. For this reason, cases of patients with imaging findings suggestive of COVID-19 pneumonia and an initial false negative RT-PCR test have been reported [10]. A further concern about the RT-PCR test is the delay in the availability of results. Indeed, in our experience, most of the patients who presented to the emergency department with a suspicion of COVID-19 pneumonia underwent their first radiological exam before results of the swab test were known.

As suggested in the recently published WHO (World Health Organization) advice guide for the diagnosis and management of COVID-19, chest imaging should be used for diagnostic purpose in symptomatic patients if RT-PCR is not available or its results are delayed, or in case of negative result in the presence of a high clinical suspicion of COVID-19 [11].

CXR and CT are the imaging procedures generally performed in the diagnosis of COVID-19 pneumonia. In this clinical setting, CXR is of easy use and is usually performed in the antero-posterior (AP) projection and in the supine position, using mobile CXR units in a dedicated and isolated room to reduce the risk of infection spreading [6,12]. Chest CT is performed with the high-resolution (HRCT) technique, using thin sections (<1.5 mm) and high-spatial resolution kernel to enhance lung parenchymal anatomical details, usually without contrast medium injection. However, evidences suggest a predisposition to thrombotic and thromboembolic disease in these patients [13], with pulmonary embolism (PE) being a known epiphenomenon of COVID-19 syndrome [14]. Therefore, in the appropriate clinical setting, contrast medium injection is required to rule out PE.

The reported sensitivity of CXR for COVID-19 pneumonia is relatively low in the early phase of the disease and in mild cases and it is inferior to that of RT-PCR essay at baseline (69 % versus 91 %, respectively) [15]. The rate of negative CXR at baseline tends to decrease when the interval time between the onset of symptoms and the CXR increases. In a retrospective study of 240 symptomatic patients with COVID-19 infection confirmed by RT-PCR, the rate of negative CXR was 36.7 % at 0–2 days after the onset of symptoms and 16.1 % at >9 days [16]. The diagnostic performance of CXR increases in clinical settings with high prevalence of disease as described by Schiaffino et al. in their experience based on *real-life* reporting without independent image review during COVID-19 outbreak in northern Italy [12]. CXR at admission to the emergency department showed a sensitivity of 89.0 % (95 % CI, 85.5 %–91.8 %) and a specificity of 60.6 % (95 % CI: 51.6 %–69.2 %) [12]. Therefore, bedside CXR – performed in the isolated rooms – can be efficiently used as first-line imaging modality in areas with high levels of contagion and high pre-test probability of disease, particularly in cases of shortage of RT-PCR essays or limited availability of dedicated CT scanners and/or difficulties in speeding up the CT room sanitization [12,17,18].

A high sensitivity of CT for diagnosis of COVID-19 pneumonia has been reported. In a recent meta-analysis of 6218 patients from 68 studies in and outside China, the pooled sensitivity of chest CT and RT-PCR were 94 % (95 % CI: 91–96 %) and 89 % (95 % CI: 81–94 %), respectively, for the diagnosis of COVID-19 pneumonia [19]. In another meta-analysis [20], a pooled sensitivity of 92 % (95 % CI: 86–96 %) was reported for CT in detecting COVID-19 among studies from different areas of China; the pooled sensitivity of CT was even higher (up to 99 %) in the region with more severe epidemic. Based on its high sensitivity, CT has been proposed as the primary diagnostic tool in epidemic areas, in order to early recognize suspicious cases and possibly limit the spread of infection. However, a more recent meta-analysis including 37 studies with 9610 patients underlined that the sensitivity of CT significantly decreases from 94 % to 75 % when studies with low risk of biases are included [21]. Furthermore, the possibility that CT can be normal within the first 3 days from the onset of symptoms (day 0–2) in up to 56 % of cases should be taken into consideration when assessing patients with suspected COVID-19 pneumonia [22]. CT can also detect abnormalities in asymptomatic patients, with a rate of 54 %, according to Inui S. et al. [23].

The reported specificity of CT is moderate to low; it was only 37 % (95 % CI: 26–50 %) in the meta- analysis by Kim et al. [19]. The same authors observed that in regions with a prevalence of disease <10 %, the PPV of RT-PCR was more than ten times higher than that of CT, meaning that applying CT as a screening tool in these areas could potentially lead to a large number of false-positive results, with an unjustified increase in medical costs [19]. Due to the abovementioned limitations, some authors suggest considering CT as a supplemental diagnostic tool, especially in symptomatic patients [24].

Apart from recognizing COVID-19 pneumonia features, imaging - especially CT - may reveal possible alternative diagnoses (e.g. pulmonary oedema, alveolar haemorrhage, other type of lung infections) that justify patient's respiratory symptoms [25,26]. The rule-out role of CT is also highlighted by the recent Fleischner Society consensus statement, particularly in patients manifesting with moderate-to-severe symptoms and a negative or ongoing RT-PCR test [6].

The WHO advice guide also underlined that the use of chest CT is particularly helpful in patients with known pre-existing pulmonary diseases [11].

In order to standardize the level of suspicion of COVID-19 pneumonia on CT scans, a categorical assessment scheme, the COVID-19 Reporting and Data System (CO-RADS) has been proposed, with levels ranging from very low (CO-RADS category 1) to very high suspicion (CO-RADS category 5), with a CO- RADS 6 category reserved for RT-PCR proven cases [27].

Imaging also plays a role in prognostic assessment and patient stratification in COVID-19 pneumonia. Some CXR scoring systems have been recently developed to answer these needs in the clinical practice with interesting results [28,29]. In particular, higher disease scores at baseline have been associated to hospitalization, requirement for mechanical ventilation [28] and in-hospital mortality [30].

Similarly, categorization and quantification of HRCT abnormalities in COVID-19 pneumonia have been demonstrated to correlate with development of severe disease course [31,32], ICU admission [33,34], and in-hospital mortality [34]. Particularly, Colombi et al. [35] demonstrated that patients requiring ICU admission or deceased have higher parenchymal involvement (4 or more lobes) and show less aerated lung parenchyma on baseline HRCT compared to the other patients.

The importance of chest imaging to assess disease evolution is also unquestioned. In patients requiring hospitalization, CXR is essential in guiding clinical management, as the serial evaluation allows an adequate assessment of the evolution of findings, avoiding unnecessary radiation exposures. This is especially true in critically ill patients [36] (Fig. 1), or during regression of symptoms in favourable cases.

For a late follow-up, HRCT is the modality of choice, particularly in assessing eventual persistent or fibrotic lung abnormalities. Lastly, imaging is essential in the early detection of complications, such as barotrauma, superimposed bacterial lung infections and empyema.

3. Common chest imaging findings in COVID-19 patients with pathogenesis correlation

Ground glass (GG) opacities, a *crazy paving* pattern characterized by GG opacities with superimposed septal thickening, and consolidations

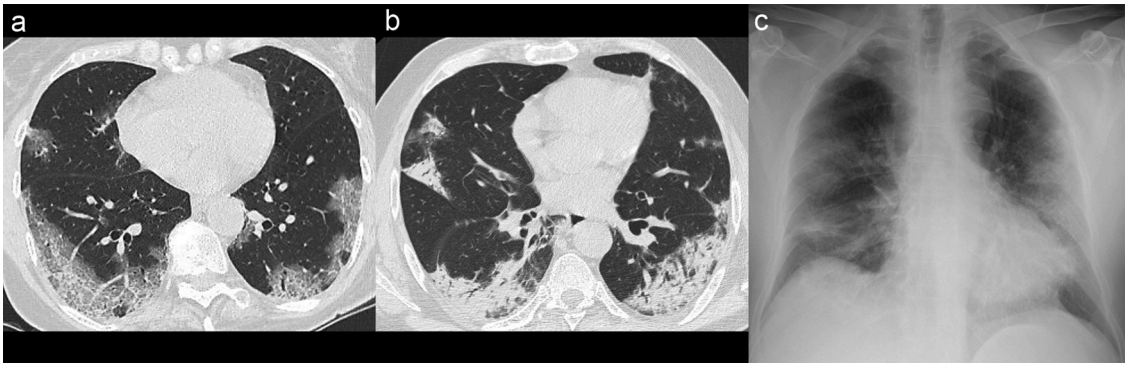

Fig. 2. Common findings of COVID-19 pneumonia in two different patients. In the first patient, the axial HRCT image (a) shows bilateral, dorsal, subpleural areas of *crazy paving*. In the second patient, the axial HRCT image (b) demonstrates patchy bilateral consolidations with subpleural and dorsal distribution, and lower lobes volume loss. Chest X-ray (CXR) (c) of the same case as in b nicely depicts the bilateral peripheral mid-basal distribution of the opacities.

are common HRCT findings in patients with COVID-19 pneumonia [37] (Fig. 2). Incidence of these findings varies among different studied populations. In a recently published meta-analysis comprising 4410 patients, GG opacities, a combination of GG opacities and consolidations, and *crazy paving* have been reported in 50.2 %, 44.4 %, and 19.5 % of cases, respectively [38].

The distribution of the above reported findings is usually bilateral and multilobar with a predominant involvement of subpleural/peripheral and posterior regions of the lungs [39]. Similar findings of GG, interstitial opacities and areas of consolidation with a peripheral and mid-basal distribution can be observed on CXR [15] (Fig. 2).

These imaging findings are the expression of a condition of acute lung injury (ALI), the main pathological pattern of the pulmonary damage caused by SARS-CoV-2, that presents with a wide spectrum of histologic patterns ranging from diffuse alveolar damage (DAD) with hyaline membrane formation to organizing pneumonia (OP) [40–42]. The predominant pathogenic mechanism of ALI induced by SARS-CoV-2 infection and shared by other coronaviruses is the angiotensin-converting enzyme 2 (ACE2) downregulation [43,44], which results in excessive inflammatory cytokine release ("*cytokine storm*") leading to apoptosis of epithelial and endothelial lung cells [45].

Direct infection of the endothelial cells and diffuse endotheliitis have been also described in several organs of COVID-19 patients, included the lungs, with subsequent oedema and parenchymal ischemia due to microvascular dysfunction [46]. Furthermore, a generalized microthrombotic injury, mediated by activation of complement pathways, has been observed within the lung microvasculature in pathologic specimens from patients deceased with severe COVID-19 pneumonia [47]. Based on these observations, microthrombosis and diffuse vascular lung injury might have a role in the pathogenesis of COVID-19 pneumonia, at least in severe and critically ill cases [47]. It has also been assumed that in some patients the parenchymal abnormalities seen at HRCT might be associated not only to inflammation or atelectasis, but also to ischemic and/or necrotic changes caused by perfusion defects [48,49].

The evolution of DAD is characterized by three sequential phases [50]. The first phase, or *exudative phase*, consists of interstitial and alveolar oedema, haemorrhage, and hyaline membrane formation, with alveolar obliteration and thickening of the inter- and intralobular septa; it has a duration of approximately 7 days. The second phase, or *proliferative phase*, consists of fibroblast proliferation within the interstitium and the alveoli, with appearance of OP foci, parenchymal remodelling and formation of reversible traction bronchiectasis and bronchiolectasis. The last *fibrotic phase* is characterized by collagen deposition with progressive and variable degree of fibrotic changes and usually starts 2 weeks after the lung injury [50]; it is potentially reversible in mild to moderate cases.

Similarly, progressive temporal stages of HRCT findings can be recognized in patients with COVID-19 pneumonia. Pan et al. have described 4 stages from initial diagnosis until patient recovery; these include an *early stage*, between 0 and 4 days from the onset of symptoms, an intermediate *progressive stage* (5–8 days) and a *peak stage*, between 9 and 13 days [51]. Starting from 2 weeks after the onset of symptoms, a gradual progressive resolution of the HRCT findings can be observed (*absorption stage*) [51]. Wang et al. confirmed this evolution, even though in their experience the absorption phase was delayed, probably because patients with more severe disease were included in their study [52].

A roughly similar appearance of the lung abnormalities in the

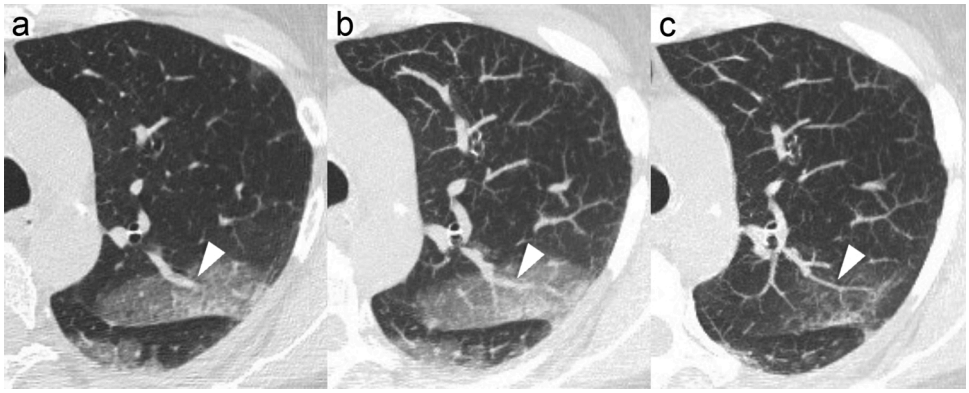

Fig. 3. Axial HRCT image (a) and maximum intensity projection (MIP) (b) in the *early phase* of COVID-19 pneumonia show enlargement (>3 mm) of a segmental pulmonary artery within the GG area in the apico- posterior segment of the left upper lobe (arrowhead in a and in b). Axial HRCT MIP image (c), performed 10 days later, shows a normal caliber of the same vessel at the same anatomical level (arrowhead in c). Note the consensual shrinkage of the focal GG area.

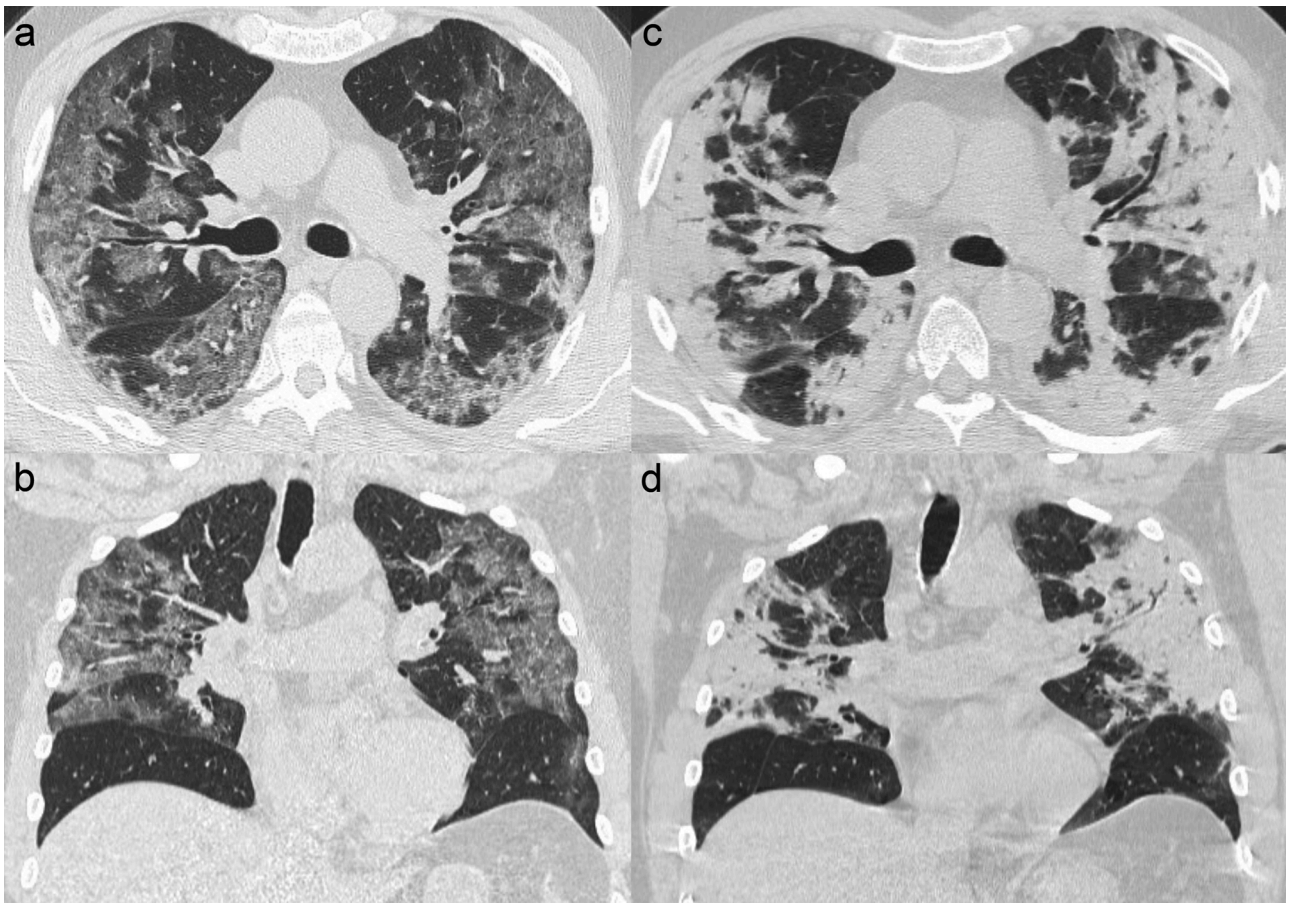

Fig. 4. Temporal evolution of COVID-19 pneumonia on HRCT. Axial (a) and coronal (b) HRCT images show bilateral GG opacities with a predominant peripheral distribution, located in the mid-upper lungs (*early phase* disease). Axial (c) and coronal (d) HRCT performed 9 days later demonstrate the typical evolution in the *progressive phase*, with extensive consolidations in the same areas previously involved by GG opacities. Note the overall mild lung volume reduction in d.

different phases of the disease is appreciable also on CXR, even though with the intrinsic limitations of this imaging modality.

The *early stage* is generally characterized by the presence of GG opacities, with the typical bilateral and multilobar distribution [39,53]; consolidations are possible, but have been described only in a minority of patients. Enlargement (greater than 3 mm in diameter) of subsegmental pulmonary vessels within the areas of GG has also been described in the early phase of COVID-19 pneumonia in up to 89 % of cases [10,37,54,55].

The aetiology of this sign is not well defined yet, although it could be related to hyperaemia and vessel wall damage induced by pro-inflammatory factors [54] or small vessel thrombosis. Some authors have indicated that this sign might be helpful in the differential diagnosis between COVID-19 and other viral pneumonia, even though it has been described in 22 % of patients with other viral non−COVID-19 pneumonia [56]. With progressive replacement of GG opacities by consolidation, the caliber of the subsegmental pulmonary vessel returns normal. It is worth noting that maximum intensity projection (MIP) reconstructions usually enhance and facilitate the identification of this sign and its evolution over time (Fig. 3).

The *progressive stage* of COVID-19 pneumonia is characterized by a more extensive lung involvement and more varied imaging features [51, 53]. GG opacities increase in density and can appear diffuse or with a *crazy paving* pattern on HRCT. Consolidations can progressively develop in the areas of GG or increase in size and number respect to previous HRCT scans [53]. Usually, in this phase, consolidations show patchy subpleural and peribronchovascolar distribution, which is the common appearance of the OP pattern [57] associated with the proliferative phase of DAD [40,58]. Similar changes are detectable also on CXR, confirming its role in identifying the temporal evolution of COVID-19 pneumonia till the improvement (Figs. 4 and 5).

The maximum disease burden is usually observed 10 days after the onset of symptoms (*peak* or *severe stage*). At this stage other well-known HRCT findings, such as *reversed halo sign*, *band-like opacities* and perilobular opacities appear [59]. Traction bronchiectasis and bronchiolectasis might be visible in this phase as ancillary findings within the consolidations, due to parenchymal remodelling (Fig. 6).

In patients developing acute respiratory distress syndrome (ARDS), COVID-19 pneumonia has an unfavourable prognosis [53,60]. In these patients, ARDS shows an atypical dissociation between the relatively low impairment of the lung mechanics and the severe hypoxemia [61], probably due to the concomitant microvascular injury that characterizes COVID-19 [47].

The *absorption stage* is characterized by a progressive clearance of the lungs over time. This stage may have quite long temporal course, with GG opacities, linear scarring and mild residual consolidations, still evident on HRCT after 4 weeks from the onset of symptoms [51] (Fig. 7). In this phase, a decrease in density of the opacities associated with a more extensive involvement of the lung has been described (the so called "*tinted*" *sign*), possibly due to the gradual resolution of the inflammation and progressive alveolar re-expansion [62] (Fig. 7). Traction bronchiectasis and bronchiolectasis tend to disappear with complete resolution of the opacities.

The time required for the complete clearance of lung abnormalities may reflect the severity and the extent of lung involvement. A prompt treatment of COVID-19 pneumonia has been correlated with a more rapid clearance of the HRCT findings [63]. However, it must be pointed out that lung abnormalities can be seen on HRCT even in presence of

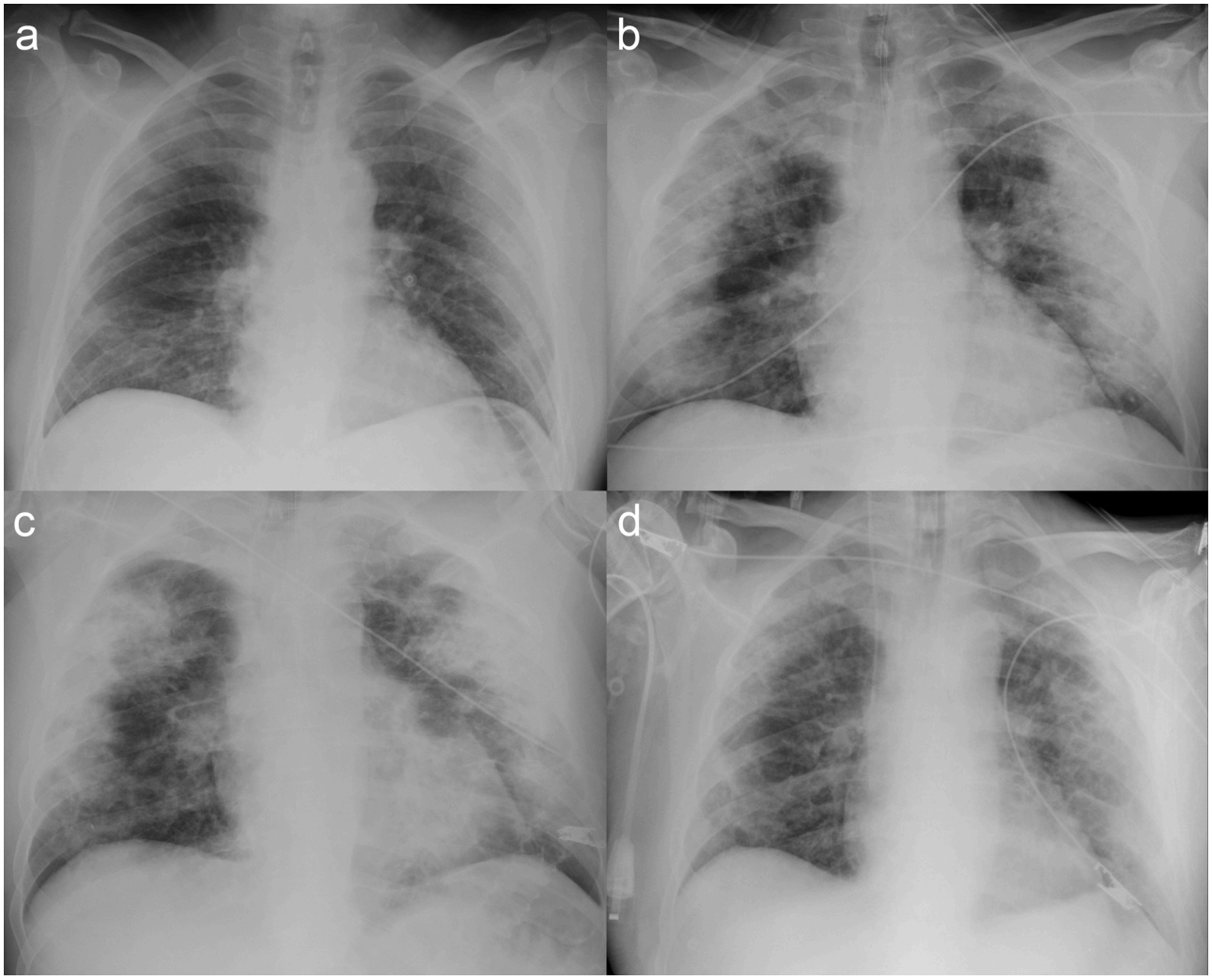

Fig. 5. Temporal evolution of COVID-19 pneumonia on chest X-ray (CXR) in the same patient as in Fig. 4. The first AP CXR (a) performed to admission in the emergency room shows ill-defined hazy opacities in the peripheral regions of both lung, especially in the left mid-zone and in the right lung base. Images (b) and (c), performed 4 and 7 days later, respectively, demonstrate a progressive increase of the opacities in terms of extension and density with progressive lung volume reduction in c. Patient experienced a clinical and radiological improvement two weeks later with reduction of lung opacities (d).

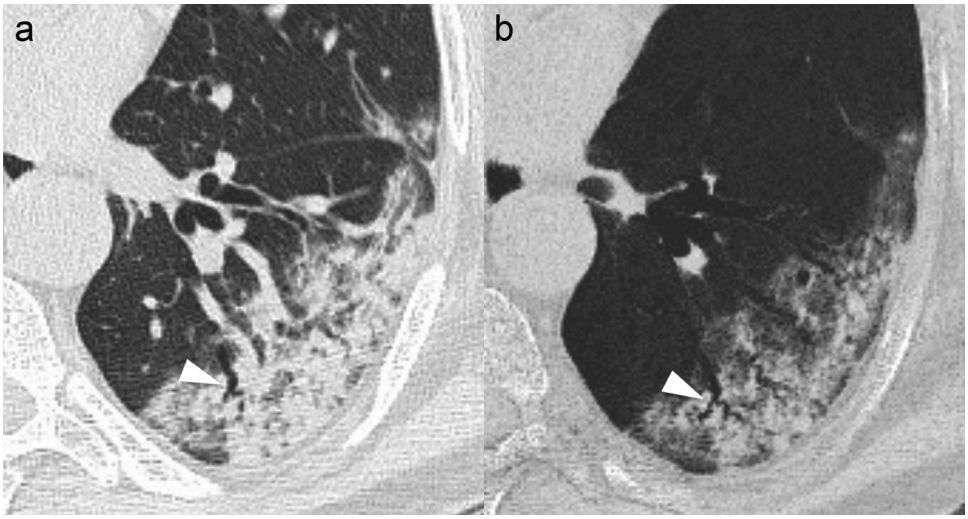

Fig. 6. Axial HRCT image (a) depicts traction bronchiectasis (arrowheads) within the peripheral area of consolidation in the left lower lobe, in a case of COVID-19 pneumonia in the *progressive phase*. The axial HRCT mIP (minimum intensity projection) image (b) enhances the visibility of traction bronchiectasis and bronchiolectasis within the same area (arrowhead).

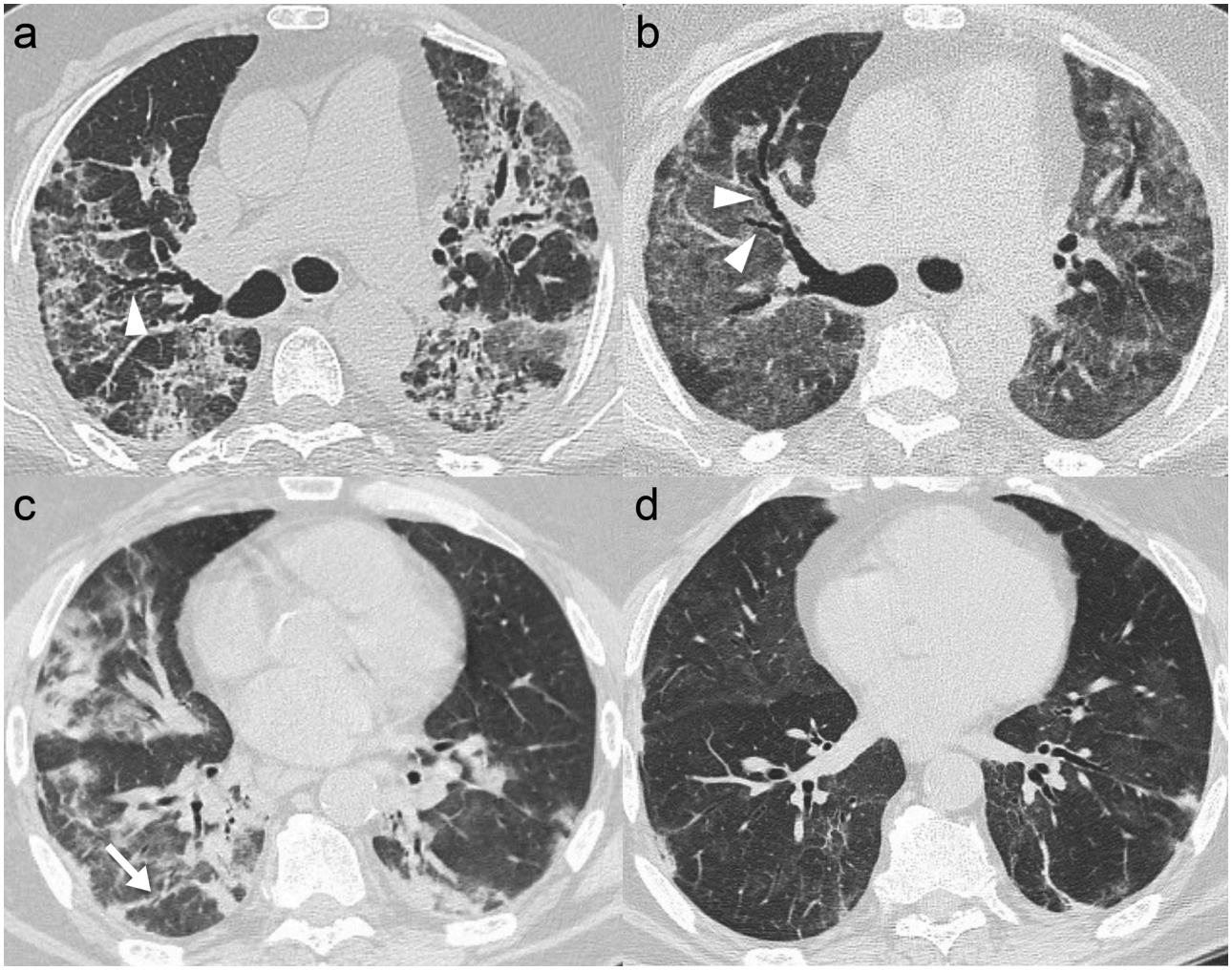

Fig. 7. Progressive (a, c) and absorption stages (b, d) on HRCT of two different patients with COVID-19 pneumonia. In the first patient, the axial HRCT image in the progressive stage (a) demonstrates areas of consolidation with mild parenchymal retraction and traction bronchiectasis (arrowhead). The axial HRCT performed 12 days later (b) shows bilateral GG opacities which are more extended than the previously detected consolidation (*"tinted" sign*). Traction bronchiectasis within the GG opacities are still present (arrowheads). These findings should always be interpreted, looking at the previous scans, as normal evolution towards the resolution of abnormalities and not as persistent or worsening disease after a complete clinical recovery. In the second patient, the axial HRCT image in the progressive stage (c) depicts consolidations, mild GG opacities and perilobular opacities (arrow), more extensive in the right lung. The axial HRCT performed 16 days later (d) demonstrates almost complete resolution of the findings, with some residual faint ill-defined GG areas and linear opacities.

complete clinical recovery and negative RT-PCR swab test [64] (Fig. 7).

Due to the young history of this outbreak, data about the morphological characteristics and potential long-term lung abnormalities in survivors from clinically significant COVID-19 disease are lacking [65]. However, the evolution of DAD, particularly in patients who recovered after full-blown ARDS [66], may lead to lung fibrosis [57], which has been demonstrated on COVID-19 pneumonia pathological specimens [67]. Therefore, a clinical and radiological follow-up might be required in order to identify and monitor potentially progressive lung fibrotic changes with the typical HRCT findings of irregular interstitial thickening, traction bronchiectasis/ bronchiolectasis, coarse reticulation, and parenchymal bands [68]. The duration and timing of follow-up with CT scans have not been defined yet.

4. Uncommon chest imaging findings and atypical presentations in COVID-19 patients

Although the majority of patients present with common findings and typical manifestations of COVID-19 pneumonia, uncommon features and atypical presentations are possible and can potentially represent a diagnostic challenge [18].

Variable rates of possible uncommon findings in different patient populations have been reported. In this section, the results of recent systematic reviews and meta-analyses are presented [37–39].

When considering the distribution of parenchymal abnormalities, unilateral lesions can be observed, especially immediately after the onset of symptoms or in pauci/asymptomatic patients [36,69] and has been described in 18.7 % of cases in a meta-analysis of 34 studies including 4121 patients [39]. In the same meta- analysis, involvement of a single lobe and predominant involvement of the anterior lung zone with relative sparing of the posterior ones have been reported in 14.9 % and 20.5 % of cases, respectively [39]. A peribronchovascular distribution of lung abnormalities has been found in only 3.6 % of 3466 patients among 28 studies [37].

When considering the lesion shape, a multifocal nodular appearance, usually with irregular margins or surrounded by peripheral GG, has been documented in 7.8 % in a meta-analysis of 45 studies including 4410 patients [38].

Enlargement of mediastinal lymph nodes has been reported in 5.1–5.4 % of cases [37–39] in patients with severe disease and extensive bilateral consolidative changes. The presence of lymph node enlargement has been associated with disease severity and poor prognosis.

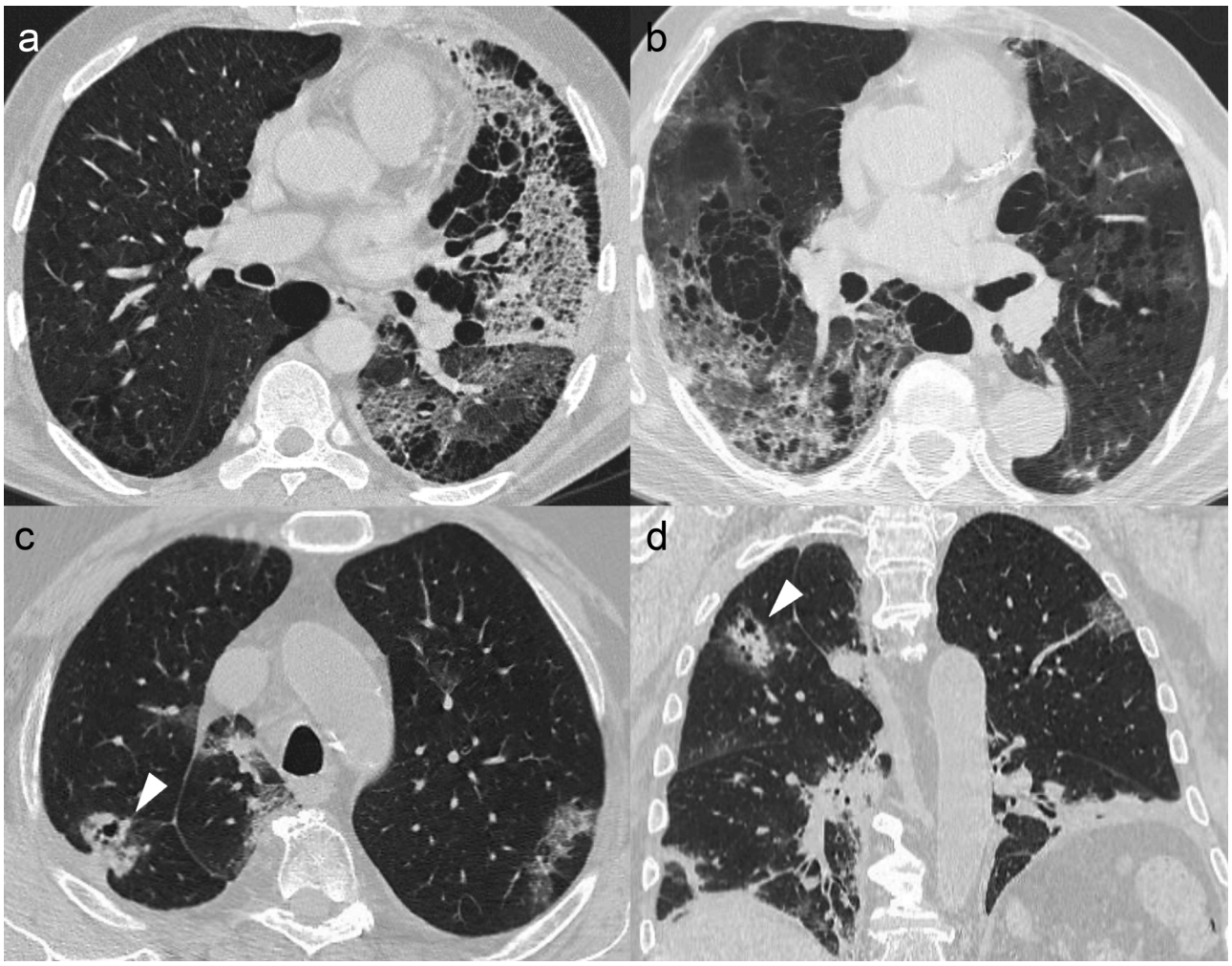

Fig. 8. Axial HRCT images (a, b) in two different patients with uncommon findings of COVID-19 pneumonia due to emphysema. In a, an uncommon unilateral GG and consolidation with subpleural sparing due to paraseptal emphysema is nicely depicted. In b, mixed GG and consolidation areas, containing apparent cystic-like changes due to centrilobular emphysema, are evident predominantly in the right lung. Axial (c) and coronal (d) HRCT images of a 77-year-old male with COVID-19 pneumonia showing bilateral subpleural and peribronchovascular consolidations with mild GG. A 3- cm, subpleural, pseudonodular, part-solid lesion with cystic-like airspaces, irregular margins, and pleural retraction is detected in the posterior segment of the right upper lobe (arrowheads); a lung adenocarcinoma was suspected on the basis of morphological features and confirmed at biopsy.

Indeed, lymphadenopathies have been observed in a significantly higher number of patients (27 %) with unfavorable course of disease during hospitalization than in those discharged (14 %), according to a single center study on a cohort of 410 patients [70].

Among the uncommon findings, the occurrence of pleural effusion has been found in about 5% of cases [37–39], while pleural thickening adjacent to the parenchymal opacities is far more common [38]. Pericardial effusion has also been rarely reported, with a pooled prevalence between 2.7 % and 3.6 % [37,38]. It is worth of note that the presence of pleural and/or pericardial effusion has been related with severe clinical course and poor prognosis of COVID-19 pneumonia [71].

Another uncommon HRCT feature related to severe disease [71] is the evidence of bronchial wall thickening within the lung opacities, described in 14.5 % of cases [38], and possibly related to inflammatory bronchial wall damage and peribronchovascular interstitial oedema. HRCT findings associated with small airways disease, such as endobronchial secretions and tree-in-bud opacities, have been described in a relatively small percentage of cases (4.1 %) [37].

Cavitation is the least common finding of COVID-19 pneumonia, with a reported pooled prevalence of only 0.1 % [38].

Apart from the uncommon findings associated with COVID-19 pneumonia, it should be noted that pre-existing underlying pulmonary diseases, such as fibrosis and emphysema, may lead to atypical HRCT presentations of COVID-19 pneumonia [18]. In case of honeycombing or paraseptal emphysema, the typical subpleural distribution may be absent (Fig. 8). The occurrence of GG opacities or consolidations superimposed on extensive background emphysema may lead to a "*bubble-like*" appearance, which could be misinterpreted as lung cysts or cavitation and lead to erroneous ruling-out of COVID- 19.

On the other hand, in case of typical findings of COVID-19 pneumonia, detection of cystic changes within a focal peripheral GG or consolidation area on HRCT should raise the possibility of a concurrent lung adenocarcinoma, especially if other *red flags* (e.g. spiculated margins, pleural retraction) associated with malignancies are evident (Fig. 8).

5. Complications

Severely ill patients are more prone to develop complications. Pneumothorax is one of these, reported in 1% of cases according to Chen et al. [72] and usually occurring in case of rupture of subpleural bullae [73]. In the clinical context of COVID-19, pneumothorax may be spontaneous, with prolonged cough and respiratory distress as known risk factors, or due to barotrauma in patients requiring mechanical

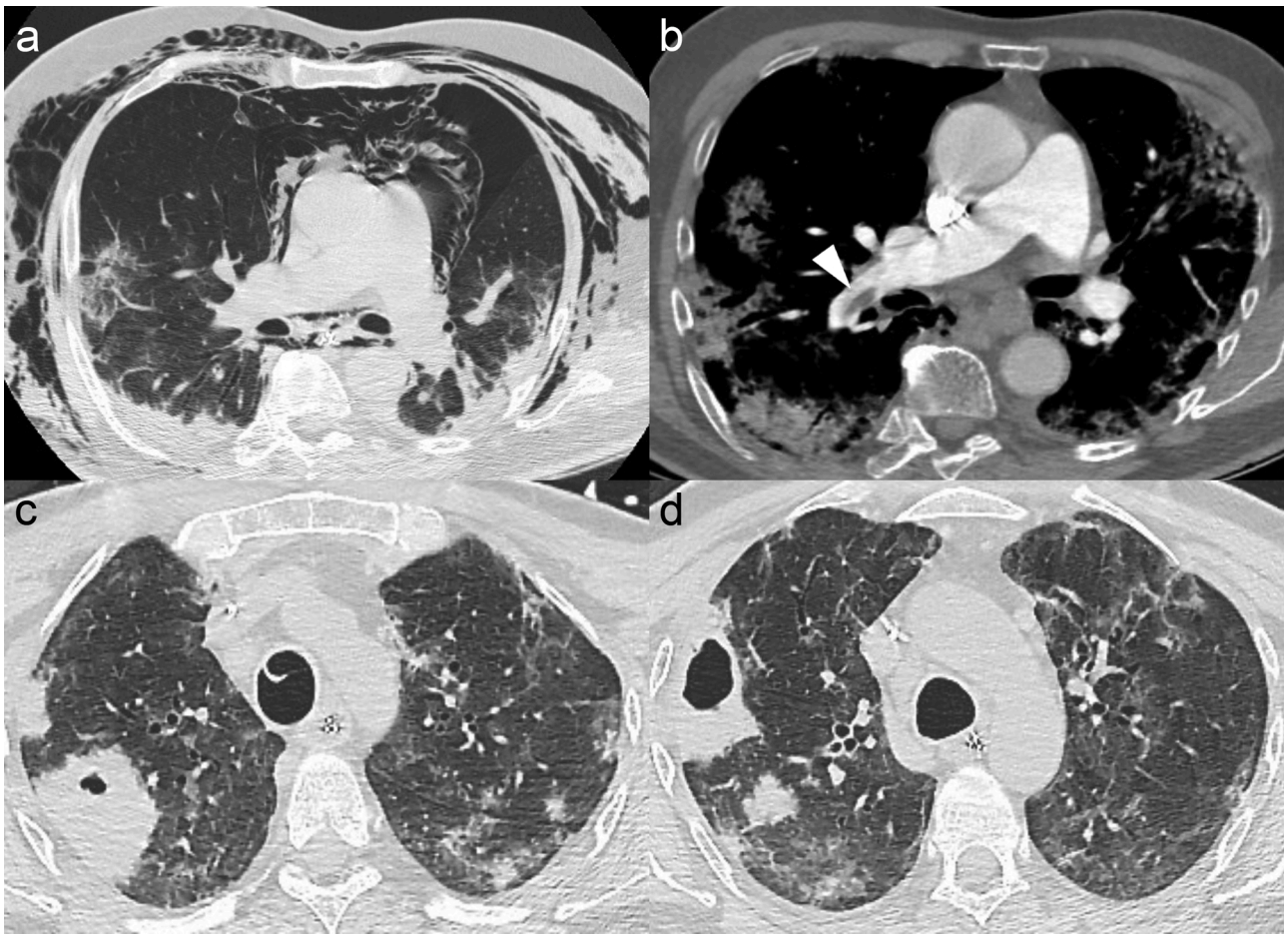

Fig. 9. Complications in two patients with severe COVID-19 pneumonia. In the first patient, axial HRCT image (a) demonstrates marked spontaneous pneumomediastinum and chest wall subcutaneous emphysema, associated with left pneumothorax. One week before, due to worsening dyspnoea, the patient had undergone CT scan with contrast medium injection to rule out pulmonary embolism (PE). Axial CT image (b) demonstrates a filling defect in the distal tract of the interlobar artery (arrowhead) due to acute PE. Note the shrinkage of the bilateral subpleural consolidations in the later CT scan (a).
In the second patient, axial HRCT images (c, d) show focal consolidations with cavitation in the right upper lobe and some small consolidations in the left lung, superimposed on diffuse GG and septal thickening. A bacterial superinfection on COVID-19 pneumonia was suspected and the bronchoalveolar lavage confirmed a *Pseudomonas aeruginosa* infection.

ventilation. Pneumomediastinum may also occur as a consequence of increased intrathoracic pressure with rupture of the alveoli, followed by air dissection through the bronchovascular bundles into the mediastinum (Macklin's effect) [74]. Subcutaneous emphysema may also be associated. Such complications must be suspected in case of sudden clinical deterioration with rapid oxygen desaturation (Fig. 9). McGuinness et al. reported an incidence of barotrauma of 15 % among COVID-19 patients requiring invasive mechanical ventilation, an incidence that was higher than the overall rate of 10 % noted in their retrospective cohort of ARDS cases [75].

The occurrence of PE has been frequently demonstrated in patients affected by COVID-19, particularly in those with more severe symptoms, and it has been considered as a part of the disease rather than a true complication [13] (Fig. 9), with an incidence of 21–30 % according to different series [14,76–79]. Based on the above, it might be potentially reasonable to perform CT scans with contrast administration in all confirmed cases of COVID-19 to assess pulmonary vessels and detect eventual arterial filling defects and lung perfusion defects on iodine map, if using a dual-source CT scanner in dual-energy mode [80]. However, in the clinical practice, the current trend is to perform CT pulmonary angiogram in cases of suspected PE due to clinical worsening, not explained by an increase of parenchymal disease burden at imaging.

Other possible complications are bacterial infections, which should be suspected in case of appearance of multiple centrilobular nodules with or without tree-in-bud opacities, and eventual cavitation within areas of consolidation superimposed to COVID-19 pneumonia lung abnormalities (Fig. 9).

6. Differential diagnosis of chest imaging findings in patients being assessed for COVID-19 pneumonia

Although in the context of the current pandemic the imaging findings described in the previous sections of this review can be indicative of COVID-19 pneumonia in areas with high prevalence of the disease, they lack in specificity and a number of disease processes both infectious and non-infectious should be considered in the differential diagnosis, as Parekh et al. have described in their recently published comprehensive review [81].

In our experience at a large tertiary metropolitan hospital in Rome during the outbreak in Italy, 1443 patients with symptoms suggestive of COVID-19 pneumonia were admitted to the emergency department between March 7 and April 27, 2020. Among them, 301 presented imaging findings indeterminate for COVID-19 or suggestive of an alternative diagnosis at the baseline CXR and underwent chest CT scanning; these patients also presented with two consecutive RT-PCR tests negative for SARS-CoV-2. In a retrospective evaluation of the final diagnosis, infectious diseases were present in 65.1 % of our patients (196/301),

Table 1
Predominant imaging findings of possible differential diagnosis with COVID-19 pneumonia occurring during outbreak.

Diagnosis			Distribution	Imaging findings	
				CXR	HRCT
Infectious	Bacterial pneumonia	Lobar pattern	lobar or nonsegmental, predominantly unilateral	- opacity - usually confined by fissure - air bronchogram common - cavitation possible - preserved lung volume	- consolidations - usually confined by fissure - air bronchogram common - cavitation possible - preserved lung volume
		Bronchopneumonia pattern	patchy/multifocal, uni- or bilateral	- nodules - confluent opacities - air bronchogram absent	- centrilobular nodules - tree-in-bud pattern - small peribronchial consolidations - lobular GG opacities - air bronchogram absent - bronchial wall thickening - mucoid impaction
		Interstitial pneumonia pattern	patchy/multifocal, subpleural and peribronchovascular, uni- or bilateral	- peribronchial thickening - interstitial opacities - interstitial-alveolar opacities	- GG opacities - consolidations - *crazy paving* - centrilobular nodules - thickening of peribronchovascular interstitium
		Nodular/ micronodular pattern	multifocal, bilateral	- nodular opacities	- well- or ill-defined nodules - *halo sign* - +/- GG opacities
	Viral pneumonia	Bronchiolar pattern	patchy/multifocal, peribronchovascular uni- or bilateral	- nodules - confluent opacities - air bronchogram absent	- centrilobular nodules - tree-in-bud pattern - small consolidations - air bronchogram absent - +/- GG opacities - bronchial wall thickening
		Interstitial pattern	patchy/multifocal, subpleural and peribronchovascular, bilateral	- interstitial opacities - reticolonodular opacities - interstitial-alveolar opacities	- GG opacities - consolidations - interlobular septal thickening - *crazy paving* - perilobular opacities - nodules possible
	Cardiogenic pulmonary edema		mid-basal lung predominance, peribronchovascular/ diffuse, bilateral	- blurring of the vessels - proximal vessel prominence - peribronchial cuffing - Kerley lines - bilateral pleural effusion	- GG opacities - smooth thickening of the interlobular septa - thickening of peribronchovascular interstitium - enlargement of pulmonary vessels - pleural effusion - mediastinal lymph node enlargement
	Acute exacerbation of fibrotic interstitial pneumonia		multifocal/diffuse, bilateral	- alveolar opacities - reticular opacities (due to underlying fibrosis) - reduced lung volume	- new GG opacities in non-fibrotic areas - fibrotic abnormalities
Non-infectious	Drug-toxicity		patchy/diffuse/multifocal, subpleural/peribronchovascular, bilateral	- interstitial opacities - alveolar opacities	- GG opacities - consolidations - perilobular opacities - +/- fibrotic abnormalities
	Aspiration		decumbent lung zones, patchy/multifocal, uni- or bilateral	- ill-defined alveolar opacities - segmental and lobar opacities	- consolidations - GG opacities - centrilobular nodules - tree-in-bud pattern - endobronchial material - abscess/cavitation/ effusion/ empyema possible - +/- pulmonary ossification
	Exogenous lipoid pneumonia		mid-basal lung predominance, patchy/multifocal, peribronchovascular	- interstitial-alveolar and/or alveolar opacities - mass-like opacities	- centrilobular GG opacities - consolidations - smooth septal thickening - *crazy paving* - fat-containing masses
	Diffuse alveolar haemorrhage		mid lung predominance, diffuse/peribronchovascular, bilateral	- alveolar opacities	- GG opacities - smooth septal thickening - *crazy paving* - ill-defined centrilobular nodules - +/- consolidations

CXR: chest X-ray; HRCT: high- resolution computed tomography; GG: ground glass.

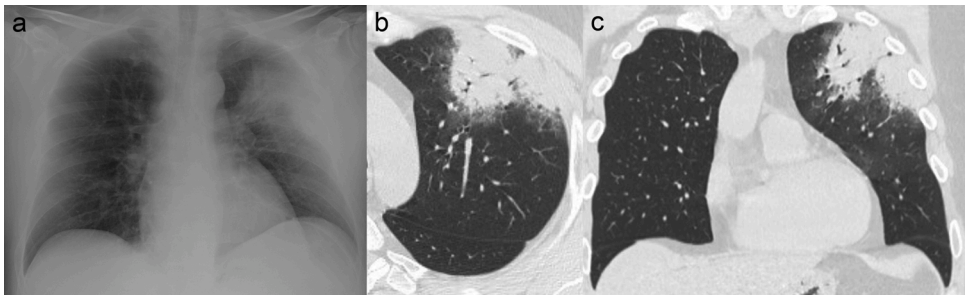

Fig. 10. 50-year-old male complaining of fever, chills and cough for 5 days. Chest X-ray (a) demonstrated a peripheral homogeneous opacity in the left upper lobe, suggestive of pneumonia with a sublobar nonsegmental appearance. Multiple RT-PCR tests resulted negative for SARS-CoV-2. Axial (b) and coronal (c) HRCT images confirm a peripheral sublobar nonsegmental consolidation with air bronchogram and mild adjacent GG in the left upper lobe. Microbiological tests were positive for *Streptococcus pneumoniae*.

with the majority caused by bacteria (56.6 %), followed by indeterminate community-acquired pneumonia (CAP) (30.1 %), viruses (7.7 %) and atypical pathogens (5.6 %). Among the remaining 105 patients with non-infectious diseases, pulmonary oedema was observed in 57 (54.2 %), followed by thoracic neoplasms (20.9 %) (progression and/or first diagnosis of primary lung cancer; metastases due to extrathoracic neoplasms), acute exacerbation of ILD (interstitial lung disease) (9.5 %), aspiration (7.6 %), ascertained drug toxicity (3.8 %), alveolar proteinosis (1.9 %), lipoid pneumonia (0.9 %) and diffuse alveolar haemorrhage (0.9 %).

The most relevant CXR and HCRT findings of possible differential diagnosis among infectious and non-infectious diseases at the time of the outbreak of COVID-19 are summarized in the Table 1.

Lower respiratory tract infections and CAP represent the most likely diagnosis in patients with fever, cough and dyspnoea, which are also common symptoms of COVID-19 pneumonia. Bacteria and viruses are the usual causative agents of CAP, even if a definite microorganism is identified in only 30 %–65 % of cases [82–84].

Bacterial pneumonia shows three possible patterns at imaging: lobar pneumonia, bronchopneumonia and interstitial pneumonia [85].

When a *lobar pneumonia pattern* is identified, the diagnosis is relatively simple and COVID-19 pneumonia can be reasonably excluded on the basis of radiological findings. Lobar pneumonia is characterized by a homogeneous lobar or nonsegmental opacity or consolidation, with or without air bronchogram, involving predominantly or exclusively one lobe. The abnormality is commonly confined by the fissure and the lung volume is preserved (Fig. 10). *Streptococcus pneumoniae*, *Legionella pneumophila* and *Mycoplasma pneumoniae* are the most common bacteria responsible of a lobar pneumonia [85]. Associated findings and/or complications include parapneumonic pleural effusion, empyema, cavitation, and lung abscess formation [85,86]. The unilobar distribution and the presence of associated findings are helpful in differentiating a bacterial pneumonia from COVID-19.

In case of a *bronchopneumonia pattern,* the causative agent leads to bronchial epithelium inflammation, with ulcerations and fibrinopurulent exudate formation and spreading through the airways' walls and adjacent pulmonary lobules [85]. CXR shows multifocal patchy nodules and confluent opacities without air bronchogram. Characteristic HRCT findings are patchy nodules with centrilobular distribution and tree-in-bud appearance, confluent peribronchial focal consolidation without air bronchogram and lobular GG areas, associated with bronchial wall thickening and mucoid impaction. These features, commonly associated with *Staphylococcus aureus* and gram-negative bacteria (*Pseudomonasaeruginosa*, *Klebsiella pneumoniae*, *Haemophilus influenzae*) pneumonias, are highly suggestive of aerogenous spread of infection [85,86]. This behaviour is in contrast to COVID-19 pneumonia, which shows a prevalent subpleural distribution of findings, absence of tree- in-bud opacities and it is rarely associated with airways involvement.

Lastly, an *interstitial pneumonia pattern* can be caused by *Mycoplasma pneumoniae* and other atypical agents, which determine direct damage of the bronchioles mucosa and subsequent inflammation and oedema of the peribronchial interstitium and interlobular septa. CXR shows peribronchial thickening and bilateral interstitial and/or interstitial-alveolar opacities [85] that may mimic COVID-19 pneumonia. HRCT shows patchy lobular GG opacities and/or consolidation, centrilobular nodules, and thickening of the peribronchovascular interstitium. Single lobe involvement, the presence of centrilobular nodules and thickening of the peribronchovascular bundles are common findings in patients with Mycoplasma pneumonia and might help in the differential diagnosis with COVID-19 pneumonia [85] (Fig. 11).

A wide range of respiratory viruses is responsible for the development of pneumonia [87]. Depending on the pathogenesis of the infection and on the causative agent, *viral pneumonia* can show different imaging patterns [87]. For this reason, despite a certain degree of overlap, the awareness of the underlined pathogenic mechanisms is crucial to understand imaging findings and to address differential diagnosis when possible.

Three main different imaging patterns have been associated with viral infections: nodular/micronodular pattern, bronchiolar pattern and interstitial pattern [87].

The *nodular/micronodular pattern* is characterized by bilateral scattered multifocal nodules with well- or ill-defined margins and possible GG appearance, and it is usually determined by haematogenous viral

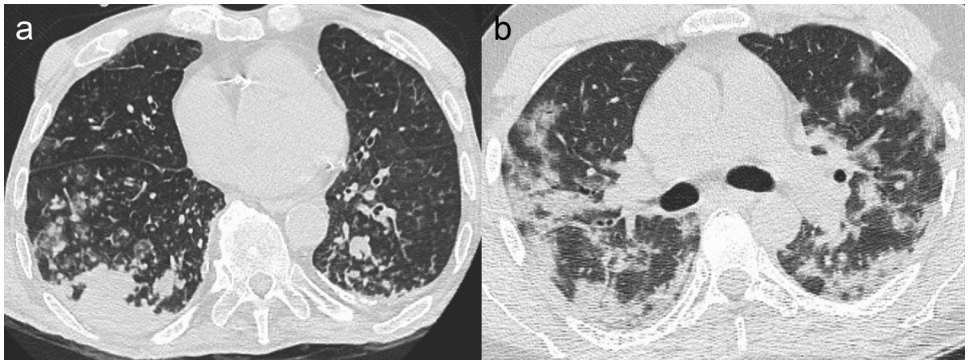

Fig. 11. Axial HRCT images (a, b) in two different patients with a diagnosis of Mycoplasma pneumonia (a) and COVID-19 pneumonia (b), respectively. In a, patchy lobular and partially confluent consolidations and GG opacities, associated with centrilobular nodules and thickening of the peribronchovascular interstitium, are evident in the lower lobes. These findings allowed a confident differential diagnosis with COVID-19 pneumonia, shown in b, characterized by mixed GG and consolidations areas with a predominant peripheral/subpleural distribution in both lungs.

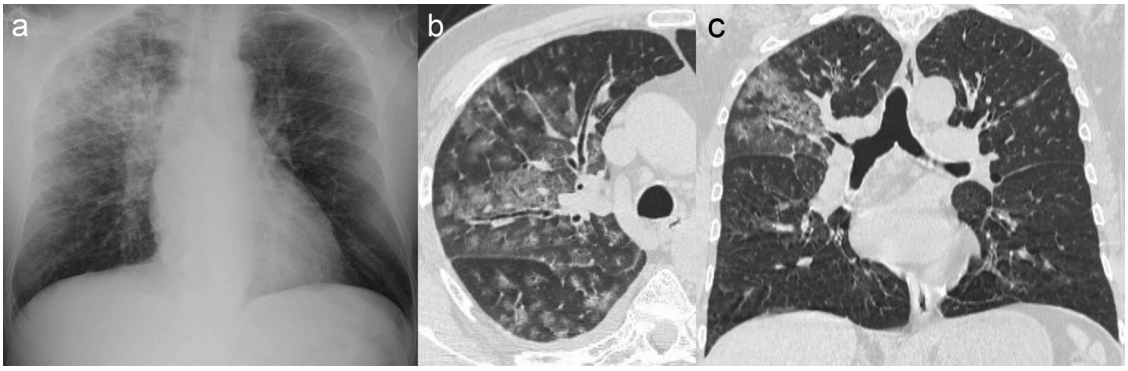

Fig. 12. 72-year-old male complaining of fever and dry cough. Chest X-ray (a) shows multiple confluent nodules and opacities in the mid-upper right lung, findings unlikely related to COVID-19 pneumonia. Axial (b) and coronal (c) HRCT images confirm the presence of multiple confluent centrilobular GG nodules and lobular areas in the right upper lobe and in the apical segment of the right lower lobe, suggestive of a bronchopneumonia pattern of infection, not related to COVID-19 pneumonia. Test was negative for SARS-CoV-2, while a diagnosis of Metapneumovirus pneumonitis was made.

spread to the alveoli, such as in Varicella-Zoster virus (VZV) pneumonia. The *bronchiolar pattern* shows an airway-centred distribution, with centrilobular nodules, tree-in-bud opacities and bronchial wall thickening, with or without peribronchovascular GG opacities and small consolidations, not dissimilar from bacterial bronchopneumonia. This pattern is due to destruction of bronchial and alveolar wall, determining small airway obstruction. It is typical of Respiratory Syncytial virus (RSV) and Human Metapneumovirus (HMPV) infections (Fig. 12); it can be also observed in Adenovirus pneumonia [87]. The *interstitial pattern* of viral pneumonia is characterized by multifocal GG opacities, interlobular septal thickening and consolidations, expression of the development of ALI with DAD [87]. This is the common imaging presentation of COVID-19 pneumonia, as discussed above (Fig. 2); however, the interstitial pattern has been also associated with other coronavirus infections, such as severe acute respiratory syndrome coronavirus (SARS-CoV-1) and Middle East respiratory syndrome coronavirus (MERS-CoV) [88,89]. SARS-CoV-2 infection is characterized by peripheral lung involvement and GG opacities more commonly than SARS-CoV-1 and MERS-CoV pneumonia, in which consolidations were prevalent [90]. Also, differently from COVID-19, SARS showed unifocal distribution in 54.6 % cases as initial presentation [91], remaining confined to a single lung in approximately one-quarter of patients [91,92]. On the other hand, when compared to COVID-19 pneumonia, a progressively extension from the lower lobe periphery into upper and perihilar lung zones was shown in MERS [92], together with a significantly higher prevalence of pleural effusion (33 %) [93].

Nevertheless, due to the shared pattern of lung damage, the differential diagnosis between COVID-19 and other interstitial viral infections is challenging [87]. In one study, a high specificity in correctly differentiating CT features of COVID-19 from other viral infections was reached, with peripheral distribution of the abnormalities, GG appearance and vessel enlargement as clue findings for differential [56]. However, due to some selection biases (e.g. low number of influenza-A cases), small cohort size and different reader's level of experience on reporting COVID- 19 cases, the observed results can be somewhat misleading [94].

Influenza pneumonia can cause bilateral reticulonodular opacities, usually with lower lobes predominance on CXR, and bilateral patchy GG opacities and consolidation, with ill-defined small nodules on HRCT [87], which can be difficult to differentiate from COVID-19 pneumonia. This is particularly true during the organizing phase of the disease when an OP pattern, commonly observed also in H1N1 influenza pneumonia, occurs [87,95]. Compared to COVID- 19, influenza demonstrates higher lower lobe predominance, with more frequent subpleural and peribronchovascular distribution of the abnormalities. Furthermore the presence of clustered and ill-defined lesions, nodules and bronchial wall thickening is more common in influenza pneumonia than in COVID-19 [96,97].

Among *non-infectious diseases* to be considered in the differential diagnosis with COVID-19 pneumonia, heart failure with *cardiogenic pulmonary oedema* is one of the most important causes of acute respiratory symptoms, especially among the elderly. On CXR, particularly in the AP projection, a differentiation between the abnormalities caused by COVID-19 and signs of pulmonary oedema may not be as easy as expected. In general, blurring of the vessels, proximal pulmonary vessel enlargement, peribronchial cuffing, evidence of bilateral Kerley lines, peribronchovascular thickening, middle-lower distribution of the opacities, and bilateral pleural effusion are typical findings that can

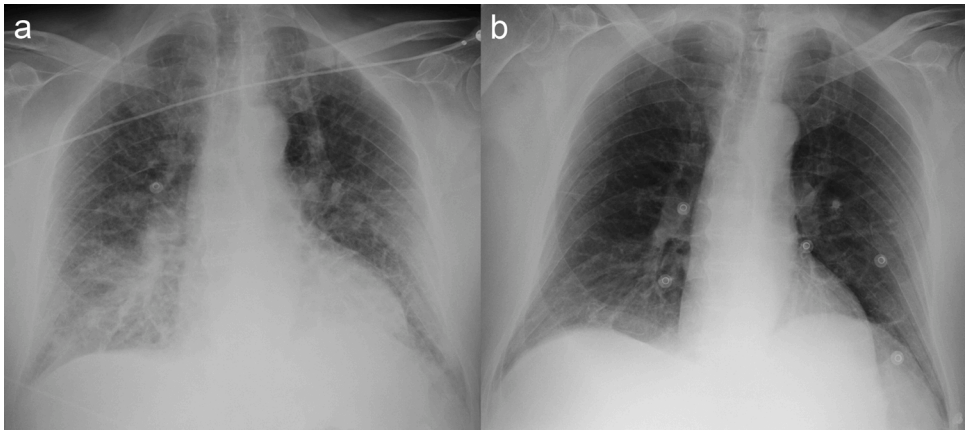

Fig. 13. 83-year-old male with history of acute coronary syndrome, complaining of severe dyspnoea and cough. The AP chest X-ray (CXR) at admission shows interstitial- alveolar opacities, with peribronchovascular and mid- basal distribution, associated with peribronchial cuffing, vessel blurring, prominence of the proximal pulmonary vessels and mild bilateral pleural effusion (a). A cardiogenic pulmonary oedema was suspected. Swab tests for COVID-19 were negative while high level of NT-proBNP (N-terminal-pro-B-type natriuretic peptide) was detected. Echocardiography showed reduced ejection fraction (35 %). The CXR performed after 5 days of treatment with diuretics demonstrates complete resolution of the pulmonary findings (b).

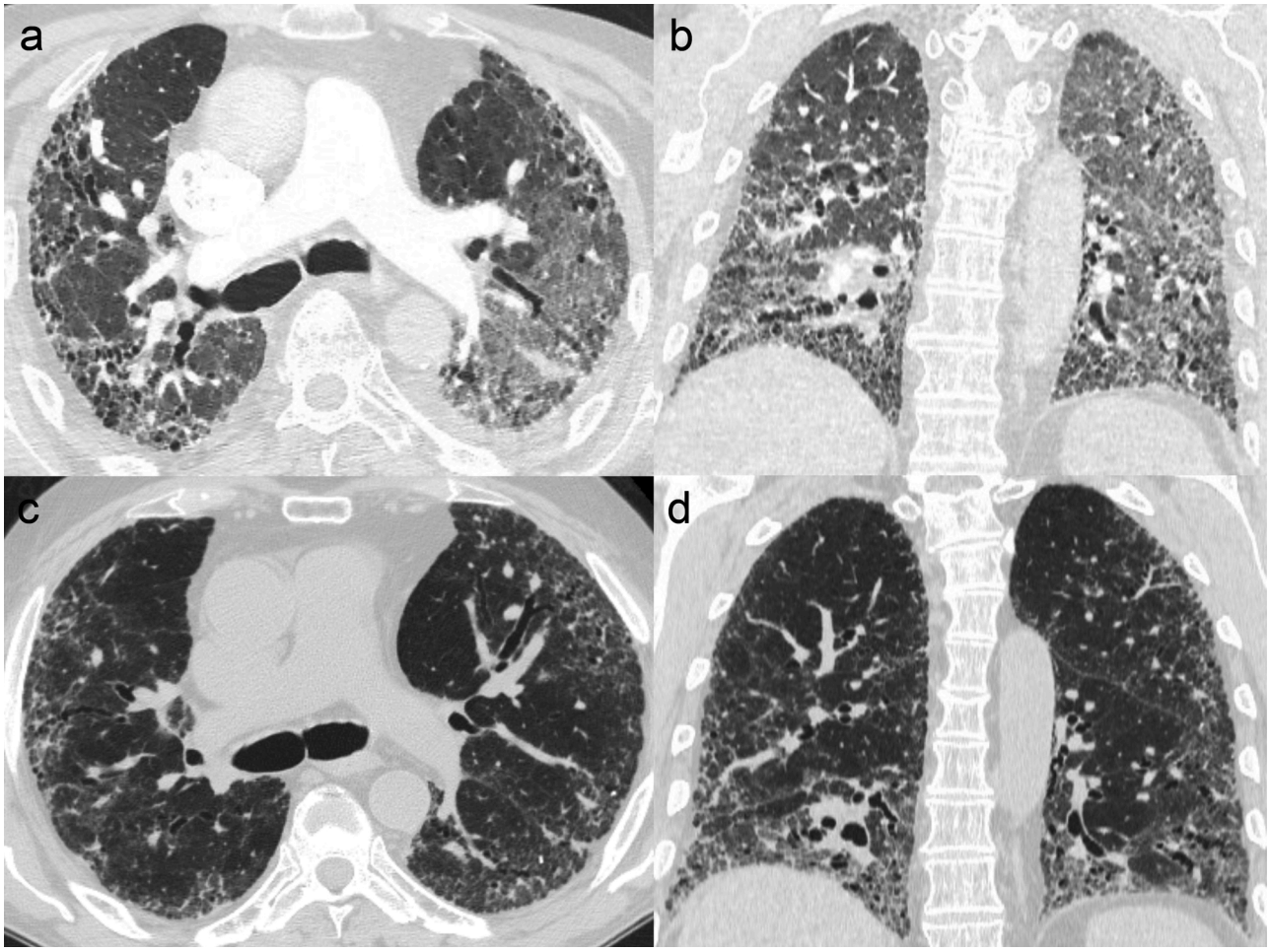

Fig. 14. 70-year-old male affected by connective tissue disease-interstitial lung disease (CTD-ILD), admitted to the emergency department with worsening dyspnoea over the last two weeks; the patient presented with diffuse bilateral *velcro- like* crackles. The HRCT scan was performed with contrast administration to rule out PE. Axial (a) and coronal (b) HRCT images show bilateral diffuse GG opacities, more evident within the left lung, in areas not extensively involved by fibrotic changes. Comparison with the HRCT exam performed one year earlier (c, d) demonstrates the new onset of diffuse GG opacities. COVID-19 swab resulted negative and a diagnosis of acute exacerbation of pulmonary fibrosis was made.

allow a confident diagnosis of pulmonary oedema, when associated with the adequate clinical context [98]. This is especially true in patients with history of cardiac disease or in presence of cardiac devices as pacemaker (Fig. 13).

On HRCT the differential diagnosis from COVID-19 is straightforward, with evidence of enlargement of the pulmonary veins, GG opacities and smooth thickening of the interlobular septa and peribronchovascular bundles, mostly with a central distribution in dependent areas, associated with pleural effusion and mediastinal lymph node enlargement [98,99].

In patients with *fibrotic interstitial pneumonia*, such as those affected by idiopathic pulmonary fibrosis (IPF), nonspecific interstitial pneumonia (NSIP) and chronic hypersensitivity pneumonitis (CHP), the onset of an *acute exacerbation* can mimic symptoms of COVID-19 pneumonia. Acute exacerbation is defined as clinical worsening of dyspnoea over the last 30 days, which can occasionally manifest with fever and flu-like symptoms [100], and is considered expression of ALI. In this context, HRCT is the modality of choice. The hallmarks are the newly appearance of bilateral GG opacities and/or consolidation occurring in the non-fibrotic areas of the lungs – usually with a multifocal or diffuse distribution – and the exclusion of alternative aetiologies, such as PE and infection, especially viral pneumonia [101,102]. Comparison with previous examinations is particularly helpful in interpreting such cases (Fig. 14).

Drug toxicity is a frequent cause of lung disease [103]. Imaging features are various, reflecting different underlying histopathology aspects. The OP pattern is a frequent manifestation of drug reaction on HRCT [103] and may mimic COVID-19 pneumonia in the progressive phase. The typical presentation of OP include bilateral, multiple, patchy consolidations with peripheral and peribronchovascular distribution and a lower lobe predominance, associated to perilobular opacities and/or *reversed halo sign* [57]. In this context, clinical data, pharmacological history and time elapsed between the start of treatment and the occurrence of symptoms are fundamental for the differential diagnosis. The NSIP pattern is another possible manifestation of drug reaction on HRCT [103] and is usually characterized by diffuse GG opacities with superimposed reticulation and mild-to-severe traction bronchiectasis/-bronchiolectasis, with a predominant bilateral lower lobe distribution [104], less likely to resemble COVID-19 pneumonia.

Aspiration with inhalation of oropharyngeal or gastric contents into the laryngeal or lower respiratory tract is probably an under-recognized cause of CAP and lung injury [105]. The risk of aspiration is increased in patients with reduced level of consciousness, abnormal cough reflex, oropharyngeal dismotility, and gastroesophageal reflux disease (GERD). The onset of symptoms can be acute or subacute, mainly depending on the aspirated content and volume [105,106]. Especially in recumbent patients, the zonal distribution can mimic that of COVID-19 pneumonia, with involvement of the posterior segments of the upper lobes and the superior and basal-posterior segments of the lower lobes. Either unilateral or bilateral lung involvement is possible [105,107]. CXR can

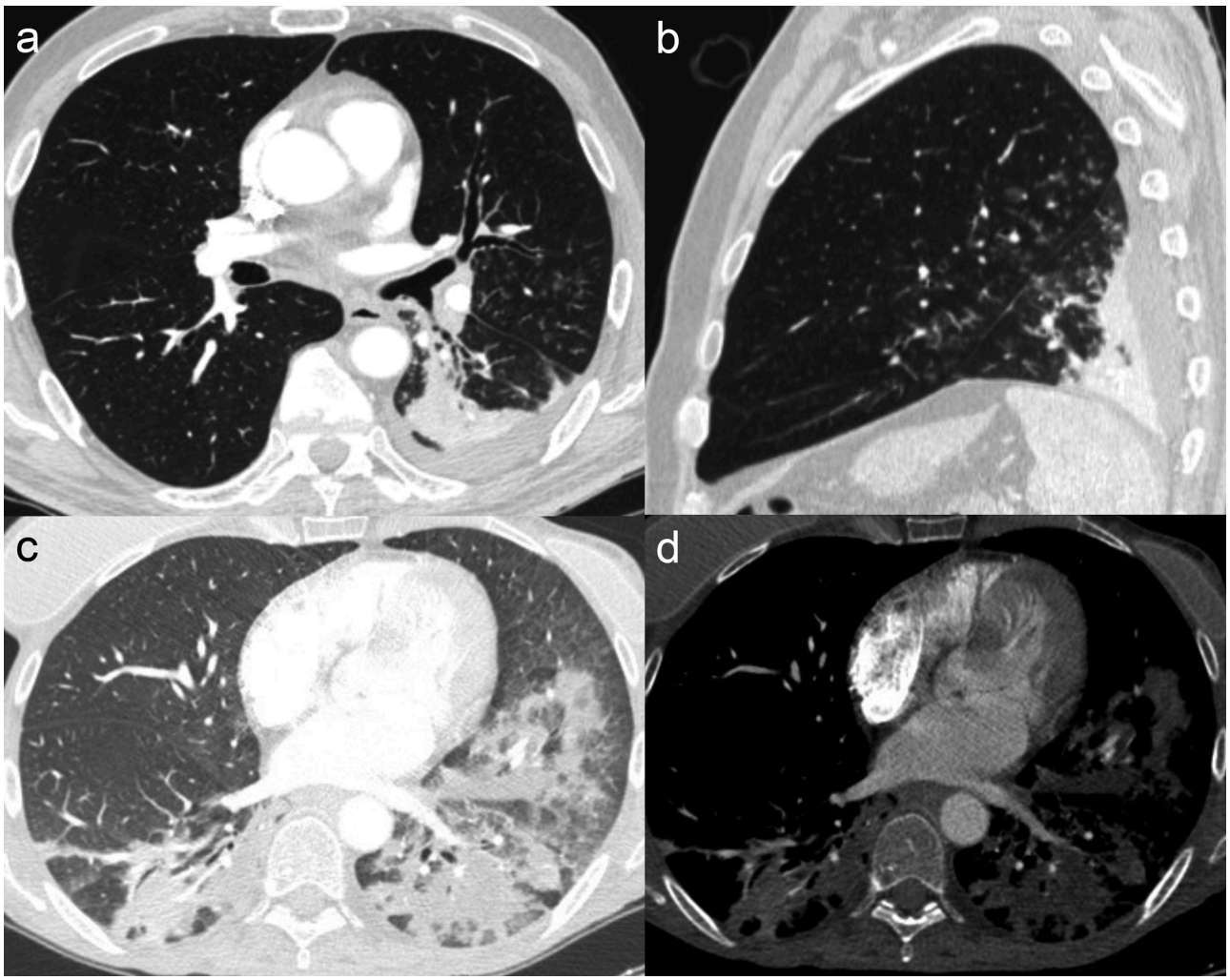

Fig. 15. HRCT images in two different patients with a diagnosis of aspiration pneumonia (a, b) and lipoid pneumonia (c, d), respectively. In the axial (a) and sagittal (b) images, a decumbent consolidation in the left lower lobe, associated with centrilobular micronodules and tree-in-bud opacities in the same lobe and in dorsal regions of the left upper lobe, is presented in a recumbent patient with recent tracheostomy. Note the left parapneumonic pleural effusion, which is an uncommon finding in COVID-19 pneumonia. In c, predominant peribronchovascular consolidations associated with mild *crazy paving* in the lower lobes and lingula, are shown in a patient with chronic use of vaseline. Note, in the mediastinal window image (d), the low attenuation values within consolidations, indicative of fat content (-40 HU). Distribution and attenuation of consolidations allowed an easy rule out of COVID-19 pneumonia.

show central ill-defined alveolar opacities or segmental and lobar opacities, whereas HRCT demonstrates consolidation in decumbent areas and multifocal patchy GG opacities, mainly with peribronchovascular distribution [105,107], associated with centrilobular nodules and/or tree-in-bud pattern [105] (Fig. 15). Despite similarities with COVID-19 pneumonia, the evidence of aspirated material filling the airways as well as the presence of centrilobular nodules and/or tree-in-bud pattern are relevant clues for the differential diagnosis [105]. Other possible ancillary findings that may help in ruling-out COVID-19 pneumonia are abscess, cavitation, parapneumonic effusion and empyema, or the presence of pulmonary ossification in a dendriform or nodular pattern (expression of underlying chronic aspiration) [105].

In case of aspiration of lipoid material, *exogenous lipoid pneumonia* can occur. Acute aspiration of large volumes of mineral oil (*fire-eater* pneumonia) [107] can have a clinical presentation similar to pneumonia, while chronic aspiration (animal fats, mineral or vegetable oils) is characterized by insidious symptoms [108]. HRCT depicts centrilobular GG opacities or multiple consolidations with a peribronchovascular distribution, mainly involving the lower lobes. Also, interlobular septal thickening and patchy multifocal areas of *crazy paving* pattern can be seen [105,108]. Moreover, the presence of consolidations or mass-like opacities with attenuation values <–10 HU (Hounsfied Unit) is diagnostic of lipoid pneumonia and can be seen in both the acute and chronic setting [105,108] (Fig. 15). Despite a typical peribronchovascular distribution of the abnormalities, in the absence of fat-containing masses, a definite exclusion of COVID-19 pneumonia is not always possible based on imaging features alone.

Diffuse alveolar haemorrhage (DAH) is another potential clinical entity which we could face in the epidemic phase of SARS-CoV2. DAH is associated with pulmonary vasculitis or connective tissue diseases among the others; haemoptysis is usually, but not always, present. CXR shows diffuse alveolar opacities, usually in the mid-zone lungs with subpleural and apical sparing, along the bronchovascular bundles. At HRCT, bilateral peribronchovascular GG opacities and smooth septal thickening are visible, with possible coexistent *crazy paving,* ill-defined centrilobular nodules and consolidations, in case of complete alveolar filling by blood [109] (Fig. 16). The peribronchovascular distribution makes the diagnosis of COVID-19 pneumonia less likely.

In the clinical practice, the differential diagnosis between COVID-19 vs non−COVID-19 patients on HRCT remains a critical task due to the overlap of imaging findings. A recently published study demonstrated that use of a simple scoring system based on seven common HRCT

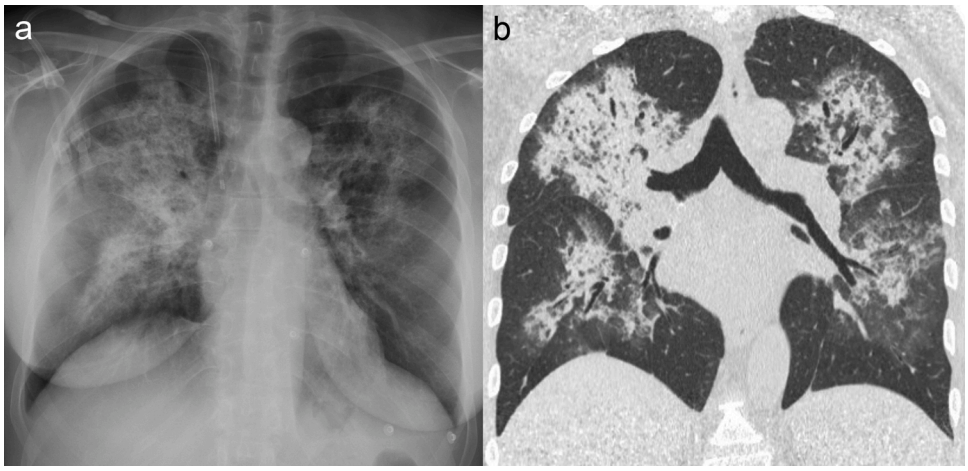

Fig. 16. 62-year-old female affected by granulomatosis with polyangiitis (GPA) and chronic renal failure (note the ultrafiltration catheter on the right) admitted to the emergency department because of progressive shortness of breath over the last few days. Haemoptysis was not reported. AP chest X-ray (CXR) (a) demonstrates bilateral ill-defined opacities (more diffuse on the right), with peribronchovascular distribution and sparing of subpleural regions, apices and bases. Coronal HRCT image (b) shows bilateral confluent consolidations with the same distribution, associated with GG opacities, ill-defined centrilobular nodules and few septal thickening. On the basis of clinical data and radiological pattern, a diagnosis of diffuse alveolar haemorrhage was made. RT-PCR essay resulted negative for SARS-CoV-2.

features (posterior part/lower lobe predilection, bilateral involvement, rounded GGO, subpleural bandlike GGO, *crazy paving* pattern, peripheral distribution, and GGO +/− consolidation) and four uncommon ones (single lobe involvement, central distribution, tree- in-bud pattern, and bronchial wall thickening) might be of help in categorizing symptomatic patients as COVID- 19 vs non−COVID-19. A high specificity (95.35 %) was achieved with a score greater than 4 [110].

However, it should be noted that imaging findings cannot provide a definite diagnosis alone and that the association with clinical and microbiological data, in a multidisciplinary context, is determinant for an accurate and rapid identification of COVID-19 positive cases.

7. Conclusions

Due to the pandemic spread of SARS-CoV-2 infection, it is essential to be familiar with common and uncommon imaging findings of COVID-19 pneumonia and their evolution over time on CXR and HRCT. CXR might be used as first-line imaging modality in the areas with high levels of contagion as well as in the serial evaluation of hospitalized and critically ill patients. On the other hand, HRCT shows a low specificity in areas with low prevalence of disease, and it should be considered the modality of choice in assessing differential diagnosis with other infectious and non- infectious lung diseases and in managing patients with pre-existing lung disease. The awareness of relationship between imaging findings and underlying pathogenesis helps radiologists to increase the level of confidence in diagnosing the disease at its first presentation, as well as in recognizing possible complications and differential diagnosis.

Declaration of competing interest

The authors declared no conflicts of interest.

Acknowledgements

The authors would like to thank Dr. Storto for her fundamental contribution to reviewing the structure and the English language of the manuscript.

References

[1] World Health Organization. Coronavirus (COVID-19). Available at: https://covid19.who.int. Updated August 06, 2020. (Accessed 6 August 2020).
[2] C. Huang, Y. Wang, X. Li, et al., Clinical features of patients infected with 2019 novel coronavirus in Wuhan, China, Lancet 395 (10223) (2020) 497–506, https://doi.org/10.1016/S0140-6736(20)30183- 5.
[3] W.J. Guan, Z.Y. Ni, Y. Hu, et al., Clinical characteristics of coronavirus disease 2019 in China, N. Engl. J. Med. 382 (18) (2020) 1708–1720, https://doi.org/10.1056/NEJMoa2002032.
[4] J.R. Lechien, C.M. Chiesa-Estomba, D.R. De Siati, et al., Olfactory and gustatory dysfunctions as a clinical presentation of mild-to-moderate forms of the coronavirus disease (COVID-19): a multicenter European study, Eur. Arch. Otorhinolaryngol. 277 (8) (2020) 2251–2261, https://doi.org/10.1007/s00405-020-05965-1.
[5] M.J. Cummings, M.R. Baldwin, D. Abrams, et al., Epidemiology, clinical course, and outcomes of critically ill adults with COVID-19 in New York City: a prospective cohort study, Lancet 395 (10239) (2020) 1763–1770, https://doi.org/10.1016/S0140-6736(20)31189- 2.
[6] Gd Rubin, Cj Ryerson, Lb Haramati, et al., The role of chest imaging in patient management during the COVID-19 pandemic: a multinational consensus statement from the Fleischner Society, Chest 158 (1) (2020) 106–116, https://doi.org/10.1016/j.chest.2020.04.003.
[7] W. Wang, Y. Xu, R. Gao, et al., Detection of SARS-CoV-2 in different types of clinical specimens, JAMA 323 (18) (2020) 1843–1844, https://doi.org/10.1001/jama.2020.3786.
[8] Y. Fang, H. Zhang, J. Xie, et al., Sensitivity of chest CT for COVID- 19: comparison to RT-PCR, Radiology 296 (2) (2020) E115–E117, https://doi.org/10.1148/radiol.2020200432.
[9] Y. Li, J. Li, et al., Stability issues of RT-PCR testing of SARS-CoV-2 for hospitalized patients clinically diagnosed with COVID-19, J. Med. Virol. 92 (7) (2020) 903–908, https://doi.org/10.1002/jmv.25786.
[10] X. Xie, Z. Zhong, W. Zhao, et al., Chest CT for typical 2019-nCoV pneumonia: relationship to negative RT-PCR testing, Radiology 296 (2) (2020) E41–E45, https://doi.org/10.1148/radiol.2020200343.
[11] E.A. Akl, I. Blazic, S. Yaacoub, et al., Use of chest imaging in the diagnosis and management of COVID-19: a WHO rapid advice guide, Radiology (2020), https://doi.org/10.1148/radiol.2020203173.
[12] S. Schiaffino, S. Tritella, A. Cozzi, et al., Diagnostic performance of chest X- Ray for COVID-19 pneumonia during the SARS-CoV-2 pandemic in Lombardy, Italy, J. Thorac. Imaging. 35 (4) (2020) W105–W106, https://doi.org/10.1097/RTI.0000000000000533.
[13] B. Bikdeli, M.V. Madhavan, D. Jimenez, et al., COVID-19 and thrombotic or thromboembolic disease: implications for prevention, antithrombotic therapy, and follow-up, J. Am. Coll. Cardiol. 75 (23) (2020) 2950–2973, https://doi.org/10.1016/j.jacc.2020.04.031.
[14] I. Leonard-Lorant, X. Delabranche, F. Severac, et al., Acute pulmonary embolism in COVID-19 patients on CT angiography and relationship to D-dimer levels, Radiology 296 (3) (2020) E189–E191, https://doi.org/10.1148/radiol.2020201561.
[15] H.Y.F. Wong, H.Y.S. Lam, A.H. Fong, et al., Frequency and distribution of chest radiographic findings in COVID-19 positive patients, Radiology 296 (2) (2020) E72–E78, https://doi.org/10.1148/radiol.2020201160.
[16] S.G. Vancheri, G. Savietto, F. Ballati, et al., Radiographic findings in 240 patients with COVID-19 pneumonia: time-dependence after the onset of symptoms, Eur. Radiol. (May 30) (2020) 1–9, https://doi.org/10.1007/s00330-020-06967-7.
[17] M. Bandirali, L.M. Sconfienza, R. Serra, et al., Chest X-ray findings in asymptomatic and minimally symptomatic quarantined patients in Codogno, Italy, Radiology 295 (3) (2020) E7, https://doi.org/10.1148/radiol.2020201102.
[18] N. Sverzellati, F. Milone, M. Balbi, How imaging should properly be used in COVID-19 outbreak: an Italian experience, Diagn. Interv. Radiol. 26 (3) (2020) 204–206, https://doi.org/10.5152/dir.2020.30320.
[19] H. Kim, H. Hong, S.H. Yoon, Diagnostic performance of CT and reverse transcriptase-polymerase chain reaction for coronavirus disease 2019: a meta-analysis, Radiology 296 (3) (2020) E145–E155, https://doi.org/10.1148/radiol.2020201343.
[20] B. Xu, Y. Xing, J. Peng, et al., Chest CT for detecting COVID-19: a systematic review and meta-analysis of diagnostic accuracy, Eur. Radiol. (May 15) (2020) 1–8, https://doi.org/10.1007/s00330-020-06934-2.
[21] J.V. Waller, I.E. Allen, K.K. Lin, et al., The limited sensitivity of chest computed tomography relative to reverse transcription polymerase chain reaction for Severe

Acute Respiratory Syndrome Coronavirus-2 infection: a systematic review on COVID-19 diagnostics, Invest. Radiol. (June 16) (2020), https://doi.org/10.1097/RLI.0000000000000700.
[22] A. Bernheim, X. Mei, M. Huang, et al., Chest CT findings in coronavirus disease-19 (COVID-19): relationship to duration of infection, Radiology 295 (3) (2020), https://doi.org/10.1148/radiol.2020200463.
[23] S. Inui, A. Fujikawa, M. Jitsu, et al., Chest CT findings in cases from the cruise ship "Diamond Princess" with coronavirus disease 2019 (COVID-19), Radiol. Cardiothorac. Imaging 2 (2) (2020), https://doi.org/10.1148/ryct.2020200110.
[24] J.V. Waller, P. Kaur, A. Tucker, et al., Diagnostic tools for coronavirus disease (COVID-19): comparing CT and RT-PCR viral nucleic acid testing, AJR Am. J. Roentgenol. (May 15) (2020) 1–5, https://doi.org/10.2214/AJR.20.23418.
[25] W. Dai, H. Zhang, J. Yu, et al., CT Imaging and differential diagnosis of COVID-19, Can. Assoc. Radiol. J. 71 (2) (2020) 195–200, https://doi.org/10.1177/0846537120913033.
[26] N. Sverzellati, G. Milanese, F. Milone, et al., Integrated radiologic algorithm for COVID-19 pandemic, J. Thorac. Imaging 35 (4) (2020) 228–233, https://doi.org/10.1097/RTI.0000000000000516.
[27] M. Prokop, W. van Everdingen, T. van Rees Vellinga, et al., CO-RADS - a categorical CT assessment scheme for patients with suspected COVID-19: definition and evaluation, Radiology 296 (2) (2020) E97–E104, https://doi.org/10.1148/radiol.2020201473.
[28] D. Toussie, N. Voutsinas, M. Finkelstein, et al., Clinical and chest radiography features determine patient outcomes in young and middle age adults with COVID-19, Radiology (May 14) (2000), https://doi.org/10.1148/radiol.2020201754.
[29] A. Borghesi, R. Maroldi, COVID-19 outbreak in Italy: experimental chest X-ray scoring system for quantifying and monitoring disease progression, Radiol. Med. 125 (5) (2020) 509–513, https://doi.org/10.1007/s11547-020-01200-3.
[30] A. Borghesi, A. Zigliani, S. Golemi, et al., Chest X-ray severity index as a predictor of in-hospital mortality in coronavirus disease 2019: a study of 302 patients from Italy, Int. J. Infect. Dis. 96 (2020) 291–293, https://doi.org/10.1016/j.ijid.2020.05.021.
[31] Z. Liu, C. Jin, C.C. Wu, et al., Association between initial chest CT or clinical features and clinical course in patients with coronavirus disease 2019 pneumonia, Korean J. Radiol. 21 (6) (2020) 736–745, https://doi.org/10.3348/kjr.2020.0171.
[32] F. Liu, Q. Zhang, C. Huang, et al., CT quantification of pneumonia lesions in early days predicts progression to severe illness in a cohort of COVID-19 patients, Theranostics 10 (12) (2020) 5613–5622, https://doi.org/10.7150/thno.45985.
[33] E. Burian, F. Jungmann, G.A. Kaissis, et al., Intensive care risk estimation in COVID-19 pneumonia based on clinical and imaging parameters: experiences from the Munich cohort, J. Clin. Med. 9 (5) (2020) 1514, https://doi.org/10.3390/jcm9051514.
[34] Q. Yu, Y. Wang, S. Huang, et al., Multicenter cohort study demonstrates more consolidation in upper lungs on initial CT increases the risk of adverse clinical outcome in COVID-19 patients, Theranostics 10 (12) (2020) 5641–5648, https://doi.org/10.7150/thno.46465.
[35] D. Colombi, F.C. Bodini, M. Petrini, et al., Well-aerated lung on admitting chest CT to predict adverse outcome in COVID-19 pneumonia, Radiology 296 (2) (2020) E86–E96, https://doi.org/10.1148/radiol.2020201433.
[36] M.P. Revel, A.P. Parkar, H. Prosch, et al., COVID-19 patients and the radiology department - advice from the European Society of Radiology (ESR) and the European Society of Thoracic Imaging (ESTI), Eur. Radiol. 30 (9) (2020) 4903–4909, https://doi.org/10.1007/s00330-020-06865-y.
[37] H.J.A. Adams, T.C. Kwee, D. Yakar, et al., Chest CT imaging signature of COVID-19 infection: in pursuit of the scientific evidence, Chest (June 25) (2020), https://doi.org/10.1016/j.chest.2020.06.025.
[38] V. Ojha, A. Mani, N.N. Pandey, et al., CT in coronavirus disease 2019 (COVID-19): a systematic review of chest CT findings in 4410 adult patients, Eur. Radiol. (May 30) (2020) 1–10, https://doi.org/10.1007/s00330-020-06975-7.
[39] J. Zhu, Z. Zhong, H. Li, et al., CT imaging features of 4121 patients with COVID-19: a meta-analysis, J. Med. Virol. 92 (7) (2020) 891–902, https://doi.org/10.1002/jmv.25910.
[40] S. Tian, W. Hu, L. Niu, et al., Pulmonary pathology of early-phase 2019 novel coronavirus (COVID-19) pneumonia in two patients with lung cancer, J. Thorac. Oncol. 15 (5) (2020) 700–704, https://doi.org/10.1016/j.jtho.2020.02.010.
[41] H. Zhang, P. Zhou, Y. Wei, et al., Histopathologic changes and SARS–CoV-2 immunostaining in the lung of a patient with COVID- 19, Ann. Intern. Med. 172 (9) (2020) 629–632, https://doi.org/10.7326/M20-0533.
[42] Z. Xu, L. Shi, Y. Wang, et al., Pathological findings of COVID-19 associated with acute respiratory distress syndrome, Lancet Respir. Med. 8 (4) (2020) 420–422, https://doi.org/10.1016/S2213-2600(20)30076- X.
[43] H. Xu, L. Zhong, J. Deng, et al., High expression of ACE2 receptor of 2019-nCoV on the epithelial cells of oral mucosa, Int. J. Oral Sci. 12 (1) (2020) 8, https://doi.org/10.1038/s41368-020-0074-x.
[44] Y. Imai, K. Kuba, S. Rao, et al., Angiotensin-converting enzyme 2 protects from severe acute lung failure, Nature 436 (7047) (2005) 112–116, https://doi.org/10.1038/nature03712.
[45] Q. Ye, B. Wang, J. Mao, The pathogenesis and treatment of the 'cytokine storm' in COVID-19, J. Infect. 80 (6) (2020) 607–613, https://doi.org/10.1016/j.jinf.2020.03.037.
[46] Z. Varga, A.J. Flammer, P. Steiger, et al., Endothelial cell infection and endotheliitis in COVID-19, Lancet 395 (10234) (2020) 1417–1418, https://doi.org/10.1016/S0140-6736(20)30937- 5.
[47] C. Magro, J.J. Mulvey, D. Berlin, et al., Complement associated microvascular injury and thrombosis in the pathogenesis of severe COVID-19 infection: a report of five cases, Transl. Res. 220 (2020) 1–13, https://doi.org/10.1016/j.trsl.2020.04.007. S1931-5244(20)30070- 0.
[48] S. Yin, M. Huang, D. Li, et al., Difference of coagulation features between severe pneumonia induced by SARS-CoV2 and non- SARS-CoV2, J. Thromb. Thrombolysis (April 3) (2020) 1–4, https://doi.org/10.1007/s11239-020-02105-8.
[49] N. Tang, D. Li, X. Wang, et al., Abnormal coagulation parameters are associated with poor prognosis in patients with novel coronavirus pneumonia, J. Thromb. Haemost. 18 (4) (2020) 844–847, https://doi.org/10.1111/jth.14768.
[50] K. Ichikado, High-resolution computed tomography findings of acute respiratory distress syndrome, acute interstitial pneumonia, and acute exacerbation of idiopathic pulmonary fibrosis, Semin. Ultrasound CT MR 35 (1) (2014) 39–46, https://doi.org/10.1053/j.sult.2013.10.007.
[51] F. Pan, T. Ye, P. Sun, et al., Time course of Llng changes at chest CT during recovery from 2019 novel coronavirus (COVID- 19) pneumonia, Radiology 295 (3) (2020) 715–721, https://doi.org/10.1148/radiol.2020200370.
[52] Y. Wang, C. Dong, Y. Hu, et al., Temporal changes of CT findings in 90 patients with COVID-19 pneumonia: a longitudinal study, Radiology 296 (2) (2020) E55–E64, https://doi.org/10.1148/radiol.2020200843.
[53] S. Salehi, A. Abedi, S. Balakrishnan, A. Gholamrezanezhad, Coronavirus Disease 2019 (COVID-19): A systematic review of imaging findings in 919 patients, AJR Am. J. Roentgenol. 215 (1) (2020) 87–93, https://doi.org/10.2214/AJR.20.23034.
[54] Z. Ye, Y. Zhang, Y. Wang, et al., Chest CT manifestations of new coronavirus disease 2019 (COVID-19): a pictorial review, Eur. Radiol. 30 (8) (2020) 4381–4389, https://doi.org/10.1007/s00330-020-06801-0.
[55] D. Caruso, M. Zerunian, M. Polici, et al., Chest CT features of COVID-19 in Rome, Italy, Radiology 296 (2) (2020) E79–E85, https://doi.org/10.1148/radiol.2020201237.
[56] H.X. Bai, B. Hsieh, Z. Xiong, et al., Performance of radiologists in differentiating COVID-19 from viral pneumonia on chest CT, Radiology 296 (2) (2020) E46–E54, https://doi.org/10.1148/radiol.2020200823.
[57] S.J. Kligerman, T.J. Franks, J.R. Galvin, From the radiologic pathology archives: organization and fibrosis as a response to lung injury in diffuse alveolar damage, organizing pneumonia, and acute fibrinous and organizing pneumonia, Radiographics 33 (7) (2013) 1951–1975, https://doi.org/10.1148/rg.337130057.
[58] Y. Wu, Y. Xie, X. Wang, Longitudinal CT findings in COVID-19 pneumonia: case presenting organizing pneumonia pattern, Radiol. Cardiothorac. Imaging 2 (1) (2020), https://doi.org/10.1148/ryct.2020200031.
[59] D.M. Hansell, A.A. Bankier, H. MacMahon, et al., Fleischner Society: glossary of terms for thoracic imaging, Radiology 246 (3) (2008) 697–722, https://doi.org/10.1148/radiol.2462070712.
[60] A.R.D.S. Definition Task Force, V.M. Ranieri, G.D. Rubenfeld, et al., Acute respiratory distress syndrome: the Berlin Definition, JAMA 307 (23) (2012) 2526–2533, https://doi.org/10.1001/jama.2012.5669.
[61] L. Gattinoni, S. Coppola, M. Cressoni, et al., Covid-19 does not lead to a "typical" acute respiratory distress syndrome, Am. J. Respir. Crit. Care Med. 201 (10) (2020) 1299–1300, https://doi.org/10.1164/rccm.202003-0817LE.
[62] D. Liu, W. Zhang, F. Pan, et al., The pulmonary sequalae in discharged patients with COVID-19: a short-term observational study, Respir. Res. 21 (1) (2020) 125, https://doi.org/10.1186/s12931-020-01385- 1.
[63] G. Huang, T. Gong, G. Wang, et al., Timely diagnosis and treatment shortens the time to resolution of coronavirus disease (COVID-19) pneumonia and lowers the highest and last CT scores from sequential chest CT, AJR Am. J. Roentgenol. 215 (2) (2020) 367–373, https://doi.org/10.2214/AJR.20.23078.
[64] J. Gao, J.Q. Liu, H.J. Wen, et al., The unsynchronized changes of CT image and nucleic acid detection in COVID-19: reports the two cases from Gansu, China, Respir Res. 21 (1) (2020) 96, https://doi.org/10.1186/s12931-020-01363-7.
[65] G. Kim, M. Wang, H. Pan, et al., A health system response to COVID-19 in long term care and post-acute care: a three-phase approach, J. Am. Geriatr. Soc. 68 (6) (2020) 1155–1161, https://doi.org/10.1111/jgs.16513.
[66] F. Landi, E. Gremese, R. Bernabei, et al., Post-COVID-19 global health strategies: the need for an interdisciplinary approach, Aging Clin. Exp. Res. (June 11) (2020) 1–8, https://doi.org/10.1007/s40520-020-01616-x.
[67] T. Schaller, K. Hirschbühl, K. Burkhardt, et al., Postmortem examination of patients with COVID-19, JAMA 323 (24) (2020) 2518–2520, https://doi.org/10.1001/jama.2020.8907.
[68] M. Yu, Y. Liu, D. Xu, et al., Prediction of the development of pulmonary fibrosis using serial thin-section CT and clinical features in patients discharged after treatment for COVID-19 pneumonia, Korean J. Radiol. 21 (6) (2020) 746–755, https://doi.org/10.3348/kjr.2020.0215.
[69] H. Shi, X. Han, N. Jiang, et al., Radiological findings from 81 patients with COVID-19 pneumonia in Wuhan, China: a descriptive study, Lancet Infect. Dis. 20 (4) (2020) 425–434, https://doi.org/10.1016/S1473-3099(20)30086- 4.
[70] F. Sardanelli, A. Cozzi, L. Monfardini, et al., Association of mediastinal lymphadenopathy with COVID-19 prognosis, Lancet Infect. Dis. (June 19) (2020), https://doi.org/10.1016/S1473-3099(20)30521-1.
[71] K. Li, J. Wu, F. Wu, et al., The clinical and chest CT features associated with severe and critical COVID-19 pneumonia, Invest. Radiol. 55 (6) (2020) 327–331, https://doi.org/10.1097/RLI.0000000000000672.
[72] N. Chen, M. Zhou, X. Dong, et al., Epidemiological and clinical characteristics of 99 cases of 2019 novel coronavirus pneumonia in Wuhan, China: a descriptive study, Lancet 395 (10223) (2020) 507–513, https://doi.org/10.1016/S0140-6736(20)30211- 7.

[73] R.W. Light, Management of spontaneous pneumothorax, Am. Rev. Respir. Dis. 148 (1) (1993) 245–248, https://doi.org/10.1164/ajrccm/148.1.245.
[74] C.C. Macklin, Transport of air along sheaths of pulmonic blood vessels from alveoli to mediastinum. Clinical implications, Arch. Intern. Med. Chic. (Chic) 64 (5) (1939) 913–926.
[75] G. McGuinness, C. Zhan, N. Rosenberg, et al., High incidence of barotrauma in patients with COVID-19 infection on invasive mechanical ventilation, Radiology (July 1) (2020), https://doi.org/10.1148/radiol.2020202352.
[76] N. Poyiadi, P. Cornier, P.Y. Patel, et al., Acute pulmonary embolism and COVID-19, Radiology (May 14) (2020), https://doi.org/10.1148/radiol.2020201955.
[77] F. Bompard, H. Monnier, I. Saab, et al., Pulmonary embolism in patients with COVID-19 pneumonia, Eur. Respir. J. 56 (1) (2020) 2001365, https://doi.org/10.1183/13993003.01365-2020.
[78] F. Grillet, J. Behr, P. Calame, et al., Acute pulmonary embolism associated with COVID-19 pneumonia detected by pulmonary CT angiography, Radiology 296 (3) (2020) E186–E188, https://doi.org/10.1148/radiol.2020201544.
[79] J. Poissy, J. Goutay, M. Capln, et al., Pulmonary embolism in COVID-19 patients: awareness of an increased prevalence, Circulation 142 (2) (2020) 184–186, https://doi.org/10.1161/CIRCULATIONAHA.120.047430.
[80] M. Lang, A. Som, D. Carey, et al., Pulmonary vascular manifestations of COVID-19 pneumonia, Radiol. Cardiothoracic. Imaging 2 (3) (2020) e200277, https://doi.org/10.1148/ryct.2020200277.
[81] M. Parekh, A. Donuru, R. Balasubramanya, S. Kapur, Review of the chest CT differential diagnosis of ground-glass opacities in the COVID era, Radiology (July 7) (2020), https://doi.org/10.1148/radiol.2020202504.
[82] C. Jokinen, L. Heiskanen, H. Juvonen, et al., Microbial etiology of community-acquired pneumonia in the adult population of 4 municipalities in eastern Finland, Clin. Infect. Dis. 32 (8) (2001) 1141–1154, https://doi.org/10.1086/319746.
[83] N. Johansson, M. Kalin, A. Tiveljung-Lindell, et al., Etiology of community-acquired pneumonia: increased microbiological yield with new diagnostic methods, Clin. Infect. Dis. 50 (2) (2010) 202–209, https://doi.org/10.1086/648678.
[84] L.T. Remington, W.I. Sligl, Community-acquired pneumonia, Curr Opin Pulm Med. 20 (3) (2014) 215–224, https://doi.org/10.1097/MCP.0000000000000052.
[85] T. Franquet, Imaging of community-acquired pneumonia, J. Thorac. Imaging 33 (5) (2018) 282–294, https://doi.org/10.1097/RTI.0000000000000347.
[86] N. Tanaka, T. Matsumoto, T. Kuramitsu, et al., High resolution CT findings in community-acquired pneumonia, J. Comput. Assist. Tomogr. 20 (4) (1996) 600–608, https://doi.org/10.1097/00004728-199607000- 00019.
[87] H.J. Koo, S. Lim, J. Choe, et al., Radiographic and CT features of viral pneumonia, Radiographics 38 (3) (2018) 719–739, https://doi.org/10.1148/rg.2018170048.
[88] G.C. Ooi, P.L. Khong, N.L. Müller, et al., Severe acute respiratory syndrome: temporal lung changes at thin-section CT in 30 patients, Radiology 230 (3) (2004) 836–844, https://doi.org/10.1148/radiol.2303030853.
[89] A.M. Ajlan, R.A. Ahyad, L.G. Jamjoom, et al., Middle East respiratory syndrome coronavirus (MERS- CoV) infection: chest CT findings, AJR Am. J. Roentgenol. 203 (4) (2014) 782–787, https://doi.org/10.2214/AJR.14.13021.
[90] H.J. Koo, S.-H. Choi, H. Sung, et al., RadioGraphics update: radiographic and CT features of viral pneumonia, Radiographics 40 (4) (2020) E8–E15, https://doi.org/10.1148/rg.202020009.
[91] K.T. Wong, G.E. Antonio, D.S. Hui, et al., Severe acute respiratory syndrome: radiographic appearances and pattern of progression in 138 patients, Radiology 228 (2) (2003) 401–406, https://doi.org/10.1148/radiol.2282030593.
[92] M. Hosseiny, S. Kooraki, A. Gholamrezanezhad, et al., Radiology perspective of coronavirus disease 2019 (COVID-19): lessons from severe cute espiratory syndrome and Middle East respiratory syndrome, AJR Am. J. Roentgenol. 214 (5) (2020) 1078–1082, https://doi.org/10.2214/AJR.20.22969.
[93] K.M. Das, E.Y. Lee, M.A. Enani, et al., CT correlation with outcomes in 15 patients with acute Middle East respiratory syndrome coronavirus, AJR Am. J. Roentgenol. 204 (4) (2015) 736–742, https://doi.org/10.2214/AJR.14.13671.
[94] S. Simpson, F.U. Kay, S. Abbara, et al., Radiological Society of North America expert consensus statement on reporting chest CT findings related to COVID-19. Endorsed by the Society of Thoracic Radiology, the American College of Radiology, and RSNA, J. Thorac. Imaging 35 (4) (2020) 219–227, https://doi.org/10.1097/RTI.0000000000000524.
[95] A.M. Ajlan, B. Quiney, S. Nicolaou, N.L. Müller, Swine-origin influenza A (H1N1) viral infection: radiographic and CT findings, AJR Am. J. Roentgenol. 193 (6) (2009) 1494–1499, https://doi.org/10.2214/AJR.09.3625.
[96] H. Wang, R. Wei, G. Rao, et al., Characteristic CT findings distinguishing 2019 novel coronavirus disease (COVID- 19) from influenza pneumonia, Eur. Radiol. 30 (9) (2020) 4910–4917, https://doi.org/10.1007/s00330-020-06880-z.
[97] M. Liu, W. Zeng, Y. Wen, et al., COVID-19 pneumonia: CT findings of 122 patients and differentiation from influenza pneumonia, Eur. Radiol. (May 12) (2020) 1–7, https://doi.org/10.1007/s00330-020-06928-0.
[98] T. Gluecker, P. Capasso, P. Schnyder, et al., Clinical and radiologic features of pulmonary edema, Radiographics 19 (6) (1999) 1507–1531, https://doi.org/10.1148/radiographics.19.6.g99no211507.
[99] M.L. Storto, S.T. Kee, J.A. Golden, W.R. Webb, Hydrostatic pulmonary edema: high- resolution CT findings, AJR Am. J. Roentgenol. 165 (4) (1995) 817–820, https://doi.org/10.2214/ajr.165.4.7676973.
[100] Y. Kondoh, V. Cottin, K.K. Brown, Recent lessons learned in the management of acute exacerbation of idiopathic pulmonary fibrosis, Eur. Respir. Rev. 26 (145) (2017) 170050, https://doi.org/10.1183/16000617.0050-2017.
[101] H.R. Collard, C.R. Reyrson, T.J. Corte, et al., Acute exacerbation of idiopathic pulmonary fibrosis an international working group report, Am. J. Respir. Crit. Care Med. 194 (3) (2016) 265–275, https://doi.org/10.1164/rccm.201604-0801CI.
[102] T. Ishiguro, Y. Kobayashi, R. Uozumi, et al., Viral pneumonia requiring differentiation from acute and progressive diffuse interstitial lung diseases, Intern. Med. 58 (24) (2019) 3509–3519, https://doi.org/10.2169/internalmedicine.2696- 19.
[103] S.E. Rossi, J.J. Erasmus, H.P. McAdams, et al., Pulmonary drug toxicity: radiologic and pathologic manifestations, Radiographics 20 (5) (2000) 1245–1259, https://doi.org/10.1148/radiographics.20.5.g00se081245.
[104] S.J. Kligerman, S. Groshong, K.K. Brown, D.A. Lynch, Nonspecific interstitial pneumonia: radiologic, clinical, and pathologic considerations, Radiographics 29 (1) (2009) 73–87, https://doi.org/10.1148/rg.291085096.
[105] A.D. Prather, T.R. Smith, D.M. Poletto, et al., Aspiration-related lung diseases, J. Thorac. Imaging 29 (5) (2014) 304–309, https://doi.org/10.1097/RTI.0000000000000092.
[106] M. Kikawada, T. Iwamoto, M. Takasaki, Aspiration and infection in the elderly: epidemiology, diagnosis and management, Drugs Aging 22 (2) (2005) 115–130, https://doi.org/10.2165/00002512-200522020- 00003.
[107] T. Franquet, A. Giménez, N. Rosón, et al., Aspiration diseases: findings, pitfalls, and differential diagnosis, Radiographics 20 (3) (2000) 673–685, https://doi.org/10.1148/radiographics.20.3.g00ma01673.
[108] S.L. Betancourt, S. Martinez-Jimenez, S.E. Rossi, et al., Lipoid pneumonia: spectrum of clinical and radiologic manifestations, AJR Am. J. Roentgenol. 194 (1) (2010) 103–109, https://doi.org/10.2214/AJR.09.3040.
[109] F.K. Cheah, M.N. Sheppard, D.M. Hansell, Computed tomography of diffuse pulmonary haemorrhage with pathological correlation, Clin. Radiol. 48 (2) (1993) 89–93, https://doi.org/10.1016/s0009-9260(05)81078- 5.
[110] L. Luo, Z. Luo, Y. Jia, et al., CT differential diagnosis of COVID- 19 and non-COVID-19 in symptomatic suspects: a practical scoring method, BMC Pulm. Med. 20 (1) (2020) 129, https://doi.org/10.1186/s12890-020-1170- 6.